Linear analysis of thermal blooming compensation instabilities in laser propagation

Jeffrey D. Barchers

Nutronics, Inc., 6525 Gunpark Dr., Suite 370-240, Boulder, Colorado 80301, USA (jbarchers@nutroninc.com)

Received March 16, 2009; accepted April 22, 2009;
posted May 20, 2009 (Doc. ID 108856); published June 22, 2009

Thermal blooming compensation instabilities are examined. The linearized system of thermal blooming compensation (TBC) equations is studied to develop parameters that characterize the stability of phase-only and full-wave (amplitude and phase) compensation for the effects of thermal blooming. The stabilizing effects of microscale wind shear are included in the analysis to provide a mechanism to stabilize the TBC equations. Stability is equated to existence of bounded solutions of the linear TBC equations, and appropriate dimensionless parameters are developed that ensure existence and uniqueness of bounded solutions to the TBC equations. Parameters characterizing stability are expressed in forms analogous to conventional scaling laws.

OCIS codes: 010.1300, 010.1080.

1. INTRODUCTION

An important problem in the control of high-energy laser beams propagated through a turbulent medium is that of thermal blooming [1–3]. The term "thermal blooming" describes the nonlinear defocusing of a beam that occurs due to the absorption of the beam's energy by the medium that induces a change in the refractive index of the medium. This defocusing effect can be quite severe, leading to a great deal of beam spread and significantly reduced on-axis intensity of the beam at the focal plane of the beam. If, in addition to thermal blooming, the random aberrations in the medium are also significant, this further reduces the on-axis intensity of the beam at the focal plane.

Adaptive optical systems have gained significant renown for their ability to compensate for the degrading effects of atmospheric turbulence on laser beam propagation [4–6]. The state of the art in adaptive optical systems continues to evolve, and a number of important advances in the understanding of the capability of adaptive optical systems for compensation of turbulence over long paths have been made recently [7–12]. The cited work focused on examination of the problem of compensation of phase aberrations that result in conditions of strong scintillation, specifically branch points in the complex field that have been found to cause a severe degradation in the performance of adaptive optical systems. Despite this recent work, the significantly more difficult problem of compensation of the effects of thermal blooming on high-energy laser propagation has not been completely addressed. It is natural to assume that one could employ an adaptive optical system to precompensate a high-energy laser beam based on measurements from some beacon beam, in much the same manner as for compensation of the effects of turbulence. If phase conjugation by means of a deformable mirror can correct for the effects of turbulence, then why not for thermal blooming as well? The result that was discovered and in fact observed experimentally in the field is quite interesting: attempting to compensate for the aberrations associated with thermal blooming using only phase compensation can cause the aberrations to increase in magnitude, leading to an instability with unbounded growth of the aberrations—the well-known phase compensation instability (PCI) [2,3,13,14].

Quite clearly, the presence of PCI poses a significant dilemma for the controlled propagation of high-energy laser beams through a turbulent medium. Given a phase measurement obtained from a wavefront sensing beacon, one cannot determine which aberrations are to be attributed to thermal blooming and which to turbulence. If the random refractive index fluctuations are so severe as to require compensation by an adaptive optical system, then one will necessarily also induce PCI in the process of attempting to compensate for the phase aberrations induced by propagation through turbulence.

Two important results were also recognized in the early work in this field. The chronology of these results is unclear, and they are discussed here in arbitrary order. The first result was that in some conditions, PCI can be mitigated by microscale wind shear along the propagation path [2,13,14]. Turbulence not only causes refractive index fluctuations along the propagation path, but of course also leads to fluctuations of the wind velocity along the propagation path. The random fluctuations of the wind velocity causes the aberrations induced by thermal blooming to lose coherence, in some cases preventing unbounded growth of the aberrations when corrected using phase conjugation. The only detailed treatment of the effect of microscale wind shear on PCI is that by Fried and Szeto [14].

The second result was that full-wave conjugation (compensation of both the amplitude and phase aberrations that are induced by propagation through a turbulent medium) was shown to be a stable means for compensation of thermal blooming [13]. At the time of this early work, no practical means for compensation of both amplitude

and phase aberrations had been developed. While nonlinear methods of full-wave conjugation such as four-wave mixing exist, the efficiency and feasibility of such methods is generally unknown and unproven for the primary applications of interest. The general approach that was desired was a means to control two phase-modulating devices, such as deformable mirrors (DMs), separated by some propagation distance, in a manner that uses one DM to redistribute the intensity of the beam to match that of the beacon beam and the second DM to then correct the phase aberrations on the outgoing beam and apply the phase conjugate of the beacon beam. Several algorithms for control of such a system were developed recently [15–19], and finally a practical means for closed loop stable control of the two deformable mirrors was developed [20]. This recent activity and development in the area of compensation of both amplitude and phase aberrations has led to a renewed interest in the subject of thermal blooming, given the early recognition of full-wave conjugation as a potential means to compensate for the effects of thermal blooming.

Several natural extensions of the past work in thermal blooming are examined in this paper. These results are obtained using a linearized model of the effects of thermal blooming. While clearly a linear treatment is only approximate, the insight gained from the results obtained is highly valuable. The first result obtained is a generalization and refinement of the treatment of the role of microscale wind shear in compensation of thermal blooming. The end result is a characterization of the conditions that are required for stable compensation of thermal blooming using phase-only compensation. This result is expressed in terms of integrals of measurable quantities over the propagation path that define requirements for the existence of stable solutions for phase compensation of the effects of thermal blooming. The integrals are related to the WISP number (wind-shear induced stabilization of PCI number) introduced by Fried and Szeto, but are more general than the WISP number and better supported by the underlying physics.

The second result is a treatment of full-wave conjugation, including the effects of microscale wind shear and time of flight on the compensation process. It is shown that time of flight can in fact destabilize full-wave conjugation (the reader should note that time of flight can destabilize phase compensation as well, however, the dominant destabilizing effect for phase compensation is the classical PCI).

It is worth noting at the outset that these general facts (i.e., mitigation of PCI by wind shear and full-wave conjugation as a stable solution of thermal blooming) had been identified in early work [13,14]. The primary contribution of this paper is that of developing a new method for analysis of stability of compensation of thermal blooming and corresponding results that allow the various effects associated with compensation of thermal blooming to be quantified via straightforward calculations, rather than having to become an expert in the complete machinery of the equations describing compensation of the effects of thermal blooming.

The paper begins in Section 2 with a treatment of the equations describing compensation of thermal blooming. The appropriate scales for the system of partial differential equations obtained are defined. Section 3 describes the linearization of the thermal blooming compensation (TBC) equations using the Rytov approximation. Section 4 develops a procedure for assessment of conditions for the existence of stable solutions of the linearized TBC equations. Section 5 provides an examination of mitigation of PCI by microscale wind shear and evaluation of the destabilization of full-wave conjugation by time of flight. Finally, in Section 6 the results obtained are summarized and directions for future work are suggested. Two appendices are included in this paper. Appendix A illustrates the use of the contraction mapping theorem to define conditions for existence and uniqueness of solutions to the TBC equations with instantaneous phase-only compensation. Appendix B describes a nonstandard application of the contraction mapping theorem that is used for analysis of the case of full-wave compensation.

2. EQUATIONS DESCRIBING COMPENSATION OF THERMAL BLOOMING

In this section, equations are provided that describe compensated propagation of high-energy laser beams. Although at first glance this section appears to provide only a review of a standard derivation, a minimal analysis is provided to introduce key scaling equations for propagation when thermal blooming has a significant impact. The equations are developed for monochromatic, continuous wave propagation. It is assumed that saturation of the medium does not occur. In scenarios in which a pulsed laser is used, the equations developed for the change in refractive index may not be appropriate due to our neglecting diffusion and saturation effects, and the assumptions used in neglecting certain terms in the wave equation developed from Maxwell's equations may no longer be reasonable. Subsection 2.A first derives the equations for laser heating of a turbulent medium. Subsection 2.B introduces the equation describing propagation of the beacon and appropriate boundary and initial conditions.

A. Equations for Laser Heating of a Turbulent Medium

One can derive from Maxwell's equations the following wave equation for propagation through a nonconducting, but nonhomogenous medium:

$$\nabla^2\mathcal{E}(\mathbf{r},z,t) + 2\,\nabla\{\mathcal{E}(\mathbf{r},z,t)\cdot\nabla\ln[n(\mathbf{r},z,t)]\} = (1/c^2)\partial_{tt}[n^2(\mathbf{r},z,t)\mathcal{E}(\mathbf{r},z,t)], \quad (1)$$

where $\mathcal{E}(\mathbf{r},z,t)$ is the electric field displacement, $\nabla=\hat{r}_x\partial_{r_x}+\hat{r}_y\partial_{r_y}+\hat{z}\partial_z$, c is the speed of light, $\mathbf{r}$ is the transverse coordinate, z is the coordinate along the axis of propagation, and t is the time variable. The refractive index $n(\mathbf{r},z,t)$ is approximately unity, but can be decomposed into the components

$$n(\mathbf{r},z,t) = 1 + n_T(\mathbf{r},z,t) + n_H(\mathbf{r},z,t) + n_2|\mathcal{E}(\mathbf{r},z,t)|^2, \quad (2)$$

where $n_T(\mathbf{r},z,t)$ are the refractive index fluctuations due to turbulence, $n_H(\mathbf{r},z,t)$ are the refractive index fluctuations induced by laser heating of the medium, and $n_2|\mathcal{E}(\mathbf{r},z,t)|^2$ is the Kerr nonlinearity. $n_T(\mathbf{r},z,t)$ is a ran-

dom function whose statistics are governed by the Kolmogorov theory. $n_H(\mathbf{r},z,t)$ is governed by an evolution equation describing the laser heating of the medium. A typical approach for modeling this process is to use the advection equation,

$$\partial_t n_H(\mathbf{r},z,t) + \mathbf{v}(z)\cdot\nabla_\perp n_H(\mathbf{r},z,t) = \alpha'(z)\beta(z)|\mathcal{E}(\mathbf{r},z,t)|^2, \tag{3}$$

where $\nabla_\perp = \hat{r}_x\partial_{r_x} + \hat{r}_y\partial_{r_y}$, $\alpha'(z)$ is the absorption coefficient in units of m^{-1}, and $\beta(z)$ is given by

$$\beta(z) = \frac{T_0 n_T}{C_p \rho_0 T(z)}\mathcal{T}(z), \tag{4}$$

where T_0 is the reference sea level temperature in degrees Kelvin, n_T is the thermal derivative of the refractive index in K^{-1}, C_p is the specific heat of the medium in J/kg/K, ρ_0 kg/m^3 is the density of the medium at sea level at the reference temperature T_0, and $\mathcal{T}(z)$ is the accumulated transmission loss due to absorption and scattering. It is convenient to define $\alpha(z) = -\alpha'(z)\beta(z)$, with $\alpha(z)$ having units of m^2/J, and write the advection equation as

$$\partial_t n_H(\mathbf{r},z,t) + \mathbf{v}(z)\cdot\nabla_\perp n_H(\mathbf{r},z,t) = -\alpha(z)|\mathcal{E}(\mathbf{r},z,t)|^2. \tag{5}$$

The advection Eq. (5) arises from the linearization of the hydrodynamic equations for air. The continuity, momentum, and energy equations are linearized with the assumption of an ideal gas, and diffusion and higher-order terms are neglected [14,21].

Further simplification of Eq. (1) begins by making the standard assumption that the wave can be modeled as the product of a rapidly oscillating component with a slowly varying envelope,

$$\mathcal{E}(\mathbf{r},z,t) = \exp(ik_0 z - i\omega t)\mathbf{E}(\mathbf{r},z,t),$$

where $k_0 = 2\pi/\lambda$ is the wavenumber and $\omega = k_0 c$ is the optical frequency. This reduces Eq. (1) to

$$\begin{aligned}&\partial_{zz}\mathbf{E}(\mathbf{r},z,t) + i2k_0\partial_z\mathbf{E}(\mathbf{r},z,t) + \nabla_\perp^2\mathbf{E}(\mathbf{r},z,t)\\ &\quad - (1/c^2)\partial_{tt}[n^2(\mathbf{r},z,t)\mathbf{E}(\mathbf{r},z,t)]\\ &\quad + 2i(k_0/c)\partial_t[n^2(\mathbf{r},z,t)\mathbf{E}(\mathbf{r},z,t)]\\ &\quad + 2\nabla_\perp[\mathbf{E}(\mathbf{r},z,t)\cdot\nabla_\perp \ln n(\mathbf{r},z,t)] + k_0^2(n^2-1)\\ &\quad \times(\mathbf{r},z,t)\mathbf{E}(\mathbf{r},z,t) = 0\end{aligned} \tag{6}$$

Equations (5) and (6) are rescaled according to the following transformations:

$$z = \zeta L_H - ct_0\tau, \quad \mathbf{r} = \bar{\rho}l_f = \bar{\rho}\sqrt{L_H/k_0}, \quad t = t_0\tau, \mathbf{v}$$

$$(z) = v_0\tilde{\mathbf{v}}(\zeta), \quad \alpha(z) = \alpha_0\tilde{\alpha}(\zeta), \quad \mathbf{E}(\mathbf{r},z,t) = E_0\mathbf{e}(\bar{\rho},\zeta,\tau),$$

$$n_H(\mathbf{r},z,t) = N_H\tilde{n}_H(\bar{\rho},\zeta,\tau), \quad n_T(\mathbf{r},z,t) = N_H\tilde{n}_T(\bar{\rho},\zeta,\tau),$$

$$n_2 = N_H\tilde{n}_2.$$

Several of the values for the fundamental scales are given by environmental considerations (i.e., they are measurable quantities), while the others were found from a nondimensional analysis of the scaled equations. The average beam power density is E_0^2. The scale α_0 is simply the average of $\alpha(z)$ over the propagation path from 0 to Z, $\alpha_0 = 1/Z\int_0^Z dz\,\alpha(z)$. The scale v_0 is defined by

$$\frac{1}{v_0} = \frac{1}{Z}\int_0^Z dz\frac{\tilde{\alpha}(z/L_H)}{v(z)}. \tag{7}$$

The above definition has been selected to provide consistency with past work in the area of thermal blooming; this consistency will be apparent shortly. The remaining scales are exposed via consideration of Eqs. (5) and (6). The scale length L_H which corresponds to the characteristic length along the propagation axis of aberrations to the envelope is found to be

$$L_H = \left(\frac{v_0}{\alpha_0 E_0^2}\frac{1}{\sqrt{k_0}}\right)^{2/3}. \tag{8}$$

The characteristic time for the equations, which corresponds to the Fresnel zone wind clearing time, is given by

$$t_0 = \frac{1}{v_0}\sqrt{\frac{L_H}{k_0}} = \left(\frac{1}{\alpha_0 v_0^2 E_0^2 k_0^2}\right)^{1/3}. \tag{9}$$

The final scale describes the amplitude of refractive index fluctuations due to laser heating [this scale balances the source and advection terms in Eq. (6)]:

$$N_H = \left(\frac{\alpha_0 E_0^2}{v_0 k_0}\right)^{2/3}. \tag{10}$$

This final scale is related to the traditional distortion number N_D. The distortion number is generally defined as a computation of the integrated number of radians of distortion accumulated along the path when considering geometric propagation of a uniform circular beam with diameter D through an absorbing medium:

$$N_D \propto k_0 E_0^2 D\int_0^Z dz\frac{\alpha(z)}{v(z)}. \tag{11}$$

The choice for the definition of v_0 is now clearer; one can see that N_H can be written as

$$N_H^{3/2} = \frac{E_0^2}{k_0}\int_0^Z dz\frac{\alpha(z)}{v(z)}, \tag{12}$$

and thus, $N_H \propto [(1/Dk_0^2)N_D]^{2/3}$. The difference between the traditional distortion number N_D and what is termed here the heating number N_H is in the description of physical processes. While N_D describes an accumulated effect over the entire propagation path, N_H describes the fundamental strength of the local effects along the propagation path.

On substitution of the above scales into Eqs. (5) and (6), the heating number and the ratio v_0/c are exposed as the natural perturbation parameter for laser propagation through a turbulent medium (under the assumption that laser-heating-induced changes in the refractive index will be the dominant contribution to changes in the envelope):

$$0 = \left[N_H \partial_{\zeta\zeta} - \frac{v_0}{c} N_H^{1/2} \partial_\zeta \partial_\tau + i2\partial_\zeta + \nabla_\perp^2 \right] \mathbf{e}(\bar{\rho},\zeta,\tau) + 2\left[-\left(\frac{v_0}{c}\right)^2 N_H \partial_{\tau\tau} + 2i\frac{v_0}{c} N_H^{1/2} \partial_\tau \right] \times \{[\tilde{n}_T(\bar{\rho},\zeta,\tau) + \tilde{n}_H(\bar{\rho},\zeta,\tau) + N_H n_2 E_0^2 |\mathbf{e}(\bar{\rho},\zeta,\tau)|^2]\mathbf{e}(\bar{\rho},\zeta,\tau)\} + 2N_H \nabla_\perp \{\mathbf{e}(\bar{\rho},\zeta,\tau)\cdot\nabla_\perp[\tilde{n}_T(\bar{\rho},\zeta,\tau) + \tilde{n}_H(\bar{\rho},\zeta,\tau) + N_H n_2 E_0^2 |\mathbf{e}(\bar{\rho},\zeta,\tau)|^2]\} + 2[\tilde{n}_T(\bar{\rho},\zeta,\tau) + \tilde{n}_H(\bar{\rho},\zeta,\tau) + N_H n_2 E_0^2 |\mathbf{e}(\bar{\rho},\zeta,\tau)|^2]\mathbf{e}(\bar{\rho},\zeta,\tau)$$

$$0 = \partial_\tau \tilde{n}_H(\bar{\rho},\zeta,\tau) + \tilde{\mathbf{v}}(\zeta)\cdot\nabla_\perp \tilde{n}_H(\bar{\rho},\zeta,\tau) + \tilde{\alpha}(\zeta)|\mathbf{e}(\bar{\rho},\zeta,\tau)|^2. \quad (13)$$

As N_H and v_0/c are typically quite small, one can neglect the related terms (equivalent to neglecting polarization coupling and the Kerr nonlinearity and using the paraxial approximation) to obtain a simplified set of equations for high-energy laser propagation through turbulence:

$$\left[\partial_\zeta - \frac{i}{2}\nabla_\perp^2 - i\tilde{n}_T(\bar{\rho},\zeta,\tau) - i\tilde{n}_H(\bar{\rho},\zeta,\tau) \right] u(\bar{\rho},\zeta,\tau) = 0, \quad (14)$$

$$\partial_\tau \tilde{n}_H(\bar{\rho},\zeta,\tau) + \tilde{\mathbf{v}}(\zeta)\cdot\nabla_\perp \tilde{n}_H(\bar{\rho},\zeta,\tau) + \tilde{\alpha}(\zeta)|u(\bar{\rho},\zeta,\tau)|^2 = 0. \quad (15)$$

This concludes the development of the equations describing laser propagation and heating of a turbulent medium.

B. Thermal Blooming Compensation Equations

Up to this point, there has been no mention of boundary or initial conditions, and the equation governing propagation of the beacon wave has not yet been introduced; these points are the subjects of this section. First, it is notationally convenient not to use the retarded frame; thus the analysis will proceed from this point using the standard frame, where $\zeta = L_H z$ and $t = t_0 \tau$. In this case the following equations describe propagation of a beacon, denoted by $u_b(\bar{\rho},\zeta,\tau)$, from a distance $\zeta = Z/L_H$ to the plane $\zeta = 0$; propagation of the high-energy laser beam, denoted by $u_H(\bar{\rho},\zeta,\tau)$, from $\zeta = 0$ to $\zeta = Z/L_H$; and evolution of the laser-heating-induced refractive index perturbations,

$$\left[\partial_\zeta - \frac{L_H}{ct_0}\partial_\tau - \frac{i}{2}\nabla_\perp^2 - i\tilde{n}_T(\bar{\rho},\zeta,\tau) - i\tilde{n}_H(\bar{\rho},\zeta,\tau) \right] u_H(\bar{\rho},\zeta,\tau) = 0, \quad (16)$$

$$\left[\partial_\zeta + \frac{L_H}{ct_0}\partial_\tau - \frac{i}{2}\nabla_\perp^2 - i\tilde{n}_T(\bar{\rho},\zeta,\tau) - i\tilde{n}_H(\bar{\rho},\zeta,\tau) \right] u_b(\bar{\rho},\zeta,\tau) = 0, \quad (17)$$

$$\partial_\tau \tilde{n}_H(\bar{\rho},\zeta,\tau) + \tilde{\mathbf{v}}(\zeta)\cdot\nabla_\perp \tilde{n}_H(\bar{\rho},\zeta,\tau) + \tilde{\alpha}(\zeta)|u_H(\bar{\rho},\zeta,\tau)|^2 = 0, \quad (18)$$

The following boundary / initial conditions complete the statement of the TBC equations:

$$u_b(\bar{\rho},\zeta = Z/L_H,\tau) = u_{b,0}(\bar{\rho},\tau), \quad \forall\ \tau > 0, \quad (19)$$

$$u_H(\bar{\rho},\zeta = 0,\tau) = \mathcal{K}[u_b(\bar{\rho},\zeta = 0,\tau)], \quad \forall\ \tau > \frac{L}{ct_0}, \quad (20)$$

$$\tilde{n}_H(\bar{\rho},\zeta,\tau = 0) = 0, \quad (21)$$

where $u_{b,0}(\bar{\rho},\tau)$ is given for all τ, and $\mathcal{K}$ is an operator representing the control system that takes measurements of the beacon beam to precompensate the high-energy laser beam.

Consider briefly the example of the use of a control system that performs instantaneous full wave conjugation, i.e., $\mathcal{K}[u_b(\bar{\rho},\zeta=0,\tau)] = u_b^*(\bar{\rho},\zeta=0,\tau)$. If one lets $c \to \infty$ (i.e., neglecting the time of flight) and applies this boundary condition, then one sees that everywhere, $u_H(\bar{\rho},\zeta,\tau) = u_b^*(\bar{\rho},\zeta,\tau)$. This implies that the beam profile due to thermal blooming evolves as if the high-energy laser beam propagates from the origin of the beacon beam at the plane $\zeta = Z/L_H$ and not from the plane $\zeta = 0$. Thus with this particular boundary condition, the three Eqs. (16)–(18) reduce to a pair of equations,

$$\left[\partial_\zeta - \frac{i}{2}\nabla_\perp^2 - i\tilde{n}_T(\bar{\rho},\zeta,\tau) - i\tilde{n}_H(\bar{\rho},\zeta,\tau) \right] u_H(\bar{\rho},\zeta,\tau) = 0, \quad (22)$$

$$\partial_\tau \tilde{n}_H(\bar{\rho},\zeta,\tau) + \tilde{\mathbf{v}}(\zeta)\cdot\nabla_\perp \tilde{n}_H(\bar{\rho},\zeta,\tau) + \tilde{\alpha}(\zeta)|u_H(\bar{\rho},\zeta,\tau)|^2 = 0, \quad (23)$$

with the boundary condition $u_H(\bar{\rho},\zeta = Z/L_H,\tau) = u_{b,0}^*(\bar{\rho},\tau)$. This point is interesting and may lead to further insight regarding compensation of thermal blooming in future work.

3. LINEARIZATION OF THE THERMAL BLOOMING COMPENSATION EQUATIONS

Linearization of the TBC equations proceeds using the Rytov approximation. Sasiela's treatment is particularly instructive and is followed here [22]. The linearization is performed only for the high-energy laser beam $u_H(\bar{\rho},\zeta,\tau)$, and the linearization of the beacon beam is seen trivially.

First, let $u_H(\bar{\rho},\zeta,\tau) = \exp[\Psi_H(\bar{\rho},\zeta,\tau)]$ to obtain the following from Eq. (16):

$$0 = \partial_\zeta \Psi_H(\bar{\rho},\zeta,\tau) - (L_H/ct_0)\partial_\tau \Psi_H(\bar{\rho},\zeta,\tau) - (i/2)[\nabla_\perp^2 \Psi_H(\bar{\rho},\zeta,\tau) + \nabla_\perp \Psi_H(\bar{\rho},\zeta,\tau)\cdot\nabla_\perp \Psi_H(\bar{\rho},\zeta,\tau)] - i\tilde{n}_T(\bar{\rho},\zeta,\tau) - i\tilde{n}_H(\bar{\rho},\zeta,\tau). \quad (24)$$

Consider the refractive index fluctuations $\tilde{n}_T(\bar{\rho},\zeta,\tau)$ and $\tilde{n}_H(\bar{\rho},\zeta,\tau)$ to be small, specifically of order δ, and thus write $\tilde{n}_T(\bar{\rho},\zeta,\tau) \to \delta\tilde{n}_T(\bar{\rho},\zeta,\tau)$ and $\tilde{n}_H(\bar{\rho},\zeta,\tau) \to \delta\tilde{n}_H(\bar{\rho},\zeta,\tau)$. Further, consider expanding $\Psi_H(\bar{\rho},\zeta,\tau)$ in powers of δ,

$$\Psi_H(\bar{\rho},\zeta,\tau) = \Psi_{H,0}(\bar{\rho},\zeta,\tau) + \delta\Psi_{H,1}(\bar{\rho},\zeta,\tau) + \delta^2\Psi_{H,2}(\bar{\boldsymbol{\rho}},\zeta,\tau) + \ldots.$$

Collecting the zeroth and first power of δ gives the equations

$$0 = \partial_\zeta \Psi_{H,0}(\bar{\rho},\zeta,\tau) - (L_H/ct_0)\partial_\tau \Psi_{H,0}(\bar{\rho},\zeta,\tau) - (i/2) \times [\nabla_\perp^2 \Psi_{H,0}(\bar{\rho},\zeta,\tau) + \nabla_\perp \Psi_{H,0}(\bar{\rho},\zeta,\tau)\cdot\nabla_\perp \Psi_{H,0}(\bar{\rho},\zeta,\tau)], \quad (25)$$

$$0 = \partial_\zeta \Psi_{H,1}(\bar{\rho},\zeta,\tau) - (L_H/ct_0)\partial_\tau \Psi_{H,1}(\bar{\rho},\zeta,\tau) - (i/2) \times[\nabla_\perp^2 \Psi_{H,1}(\bar{\rho},\zeta,\tau) + \nabla_\perp \Psi_{H,1}(\bar{\rho},\zeta,\tau)\cdot\nabla_\perp \Psi_{H,0}(\bar{\rho},\zeta,\tau)] - i\tilde{n}_T(\bar{\rho},\zeta,\tau) - i\tilde{n}_H(\bar{\rho},\zeta,\tau). \quad (26)$$

Equation (25) is trivially seen to be equivalent to the free-space paraxial wave equation having the solution $u_{H,0}(\bar{\rho},\zeta,\tau)=\exp[\Psi_{H,0}(\bar{\rho},\zeta,\tau)]$. Using the definition $\Psi_{H,1}(\bar{\rho},\zeta,\tau)=W_{H,1}(\bar{\rho},\zeta,\tau)/u_{H,0}(\bar{\rho},\zeta,\tau)$, one can transform Eqs. (25) and (26) into the following equations:

$$0 = \partial_\zeta u_{H,0}(\bar{\rho},\zeta,\tau) - (L_H/ct_0)\partial_\tau u_{H,0}(\bar{\rho},\zeta,\tau) - (i/2)\nabla_\perp^2 u_{H,0}(\bar{\rho},\zeta,\tau), \quad (27)$$

$$0 = \partial_\zeta W_{H,1}(\bar{\rho},\zeta,\tau) - (L_H/ct_0)\partial_\tau W_{H,1}(\bar{\rho},\zeta,\tau) - (i/2)\nabla_\perp^2 W_{H,1}(\bar{\rho},\zeta,\tau) - iu_{H,0}(\bar{\rho},\zeta,\tau)[\tilde{n}_T(\bar{\rho},\zeta,\tau) + \tilde{n}_H(\bar{\rho},\zeta,\tau)], \quad (28)$$

which have a trivial solution along the retarded frame for arbitrary initial conditions.

While the above equations represent linearization about an arbitrary solution to the free-space paraxial wave equation, it is of greater use for the purposes of this paper to consider linearization about plane-wave solutions, where $u_{H,0}(\bar{\rho},\zeta,\tau)=1$. Further, it is useful to break the complex wave functions $\Psi_{H,1}(\bar{\rho},\zeta,\tau)$ into the real and imaginary parts representing log-amplitude $\chi_H(\bar{\rho},\zeta,\tau)$ and phase $\phi_H(\bar{\rho},\zeta,\tau)$ fluctuations. The use of these assumptions and recognition of the similar form for the equations for the beacon beam lead to the plane wave linearized TBC equations,

$$0 = \partial_\zeta \chi_H(\bar{\rho},\zeta,\tau) - \frac{L_H}{ct_0}\partial_\tau \chi_H(\bar{\rho},\zeta,\tau) + \tfrac{1}{2}\nabla_\perp^2 \phi_H(\bar{\rho},\zeta,\tau), \quad (29)$$

$$0 = \partial_\zeta \phi_H(\bar{\rho},\zeta,\tau) - \frac{L_H}{ct_0}\partial_\tau \phi_H(\bar{\rho},\zeta,\tau) - \tfrac{1}{2}\nabla_\perp^2 \chi_H(\bar{\rho},\zeta,\tau) - \tilde{n}_T(\bar{\rho},\zeta,\tau) - \tilde{n}_H(\bar{\rho},\zeta,\tau), \quad (30)$$

$$0 = \partial_\zeta \chi_b(\bar{\rho},\zeta,\tau) + \frac{L_H}{ct_0}\partial_\tau \chi_b(\bar{\rho},\zeta,\tau) + \tfrac{1}{2}\nabla_\perp^2 \phi_b(\bar{\rho},\zeta,\tau), \quad (31)$$

$$0 = \partial_\zeta \phi_b(\bar{\rho},\zeta,\tau) + \frac{L_H}{ct_0}\partial_\tau \phi_b(\bar{\rho},\zeta,\tau) - \tfrac{1}{2}\nabla_\perp^2 \chi_b(\bar{\rho},\zeta,\tau) - \tilde{n}_T(\bar{\rho},\zeta,\tau) - \tilde{n}_H(\bar{\rho},\zeta,\tau), \quad (32)$$

$$0 = \partial_\tau \tilde{n}_H(\bar{\rho},\zeta,\tau) + \tilde{\mathbf{v}}(\zeta)\cdot\nabla_\perp \tilde{n}_H(\bar{\rho},\zeta,\tau) + 2\tilde{\alpha}(\zeta)\chi_H(\bar{\rho},\zeta,\tau), \quad (33)$$

where the final equation arises from the linearization. The boundary conditions for the linearized TBC equations are taken to be

$$\chi_b(\bar{\rho},\zeta = Z/L_H,\tau) = 0, \quad \forall\ \tau > 0, \quad (34)$$

$$\phi_b(\bar{\rho},\zeta = Z/L_H,\tau) = 0, \quad \forall\ \tau > 0, \quad (35)$$

$$\chi_H(\bar{\rho},\zeta=0,\tau) = \int_{L_H/ct_0}^{\tau} \mathrm{d}\tau' a(\tau-\tau')\chi_b(\bar{\rho},\zeta=0,\tau'), \quad \forall\ \tau > \frac{L_H}{ct_0}, \quad (36)$$

$$\phi_H(\bar{\rho},\zeta=0,\tau) = \int_{L_H/ct_0}^{\tau} \mathrm{d}\tau' p(\tau-\tau')\phi_b(\bar{\rho},\zeta=0,\tau'), \quad \forall\ \tau > \frac{L_H}{ct_0}, \quad (37)$$

$$\tilde{n}_H(\bar{\rho},\zeta,\tau=0) = 0, \quad (38)$$

where the functions $a(\tau)$ and $p(\tau)$ are taken to be linear functions that are either delta functions representing instantaneous phase conjugation, $a(\tau)=0$, $p(\tau)=-\delta(\tau)$; instantaneous full-wave conjugation, $a(\tau)=\delta(\tau)$, $p(\tau)=-\delta(\tau)$; or of the form representing a finite bandwidth compensation system,

$$a(\tau) = \omega_a \exp(-\omega_a\tau), \quad (39)$$

$$p(\tau) = -\omega_p \exp(-\omega_p\tau). \quad (40)$$

The servo bandwidths (in radians/t_0) for amplitude and phase compensation are ω_a and ω_p, respectively.

4. CONDITIONS FOR EXISTENCE OF SOLUTIONS OF THE LINEARIZED THERMAL BLOOMING COMPENSATION EQUATIONS

The approach taken in this paper to assess stability of the solutions of the linearized TBC equations is to determine conditions that guarantee the existence of solutions that are bounded for all time. In Subsection 4.A, an integral equation is developed that can be used to assess existence of solutions to the linearized TBC equations. In Subsection 4.B, this integral equation is modified to account for the microscale random variations in the wind velocity along the path.

A. Development of Integral Equation Determining Existence of Solutions for the Linearized TBC Equations

The first step is to perform Fourier and Laplace transforms of Eqs. (29)–(33), taking $\bar{\rho}\to\bar{\kappa}$ and $\tau\to s$ and noting that the initial condition (in time) for all variables is 0. The following equations are obtained:

$$0 = \partial_\zeta \chi_H(\bar{\kappa},\zeta,s) - \frac{L_H}{ct_0}s\chi_H(\bar{\kappa},\zeta,s) - \frac{\kappa^2}{2}\phi_H(\bar{\kappa},\zeta,s), \quad (41)$$

$$0 = \partial_\zeta \phi_H(\bar{\kappa},\zeta,s) - \frac{L_H}{ct_0}s\phi_H(\bar{\kappa},\zeta,s) + \frac{\kappa^2}{2}\chi_H(\bar{\kappa},\zeta,s) - \tilde{n}_T(\bar{\kappa},\zeta,s) - \tilde{n}_H(\bar{\kappa},\zeta,s), \quad (42)$$

$$0 = \partial_\zeta \chi_b(\bar{\kappa},\zeta,s) + \frac{L_H}{ct_0}s\chi_b(\bar{\kappa},\zeta,s) - \frac{\kappa^2}{2}\phi_b(\bar{\kappa},\zeta,s), \quad (43)$$

$$0 = \partial_\zeta \phi_b(\bar{\kappa},\zeta,s) + \frac{L_H}{ct_0} s\phi_b(\bar{\kappa},\zeta,s) + \frac{\kappa^2}{2}\chi_b(\bar{\kappa},\zeta,s) - \tilde{n}_T(\bar{\kappa},\zeta,s) - \tilde{n}_H(\bar{\kappa},\zeta,s), \tag{44}$$

$$0 = s\tilde{n}_H(\bar{\kappa},\zeta,s) - i\bar{\kappa}\cdot\tilde{\mathbf{v}}(\zeta)\tilde{n}_H(\bar{\kappa},\zeta,s) + 2\tilde{\alpha}(\zeta)\chi_H(\bar{\kappa},\zeta,s). \tag{45}$$

Equation (45) can be solved in transform space:

$$\tilde{n}_H(\bar{\kappa},\zeta,s) = -\frac{2\tilde{\alpha}(\zeta)\chi_H(\bar{\kappa},\zeta,s)}{s - i\bar{\kappa}\cdot\tilde{\mathbf{v}}(\zeta)}. \tag{46}$$

Equations (43) and (44) for beacon wave propagation can also be solved trivially:

$$\chi_b(\bar{\kappa},\zeta,s) = \int_\zeta^{Z/L_H} d\zeta' e^{-L_H/ct_0 s(\zeta'-\zeta)} \sin\left[\frac{\kappa^2}{2}(\zeta'-\zeta)\right][\tilde{n}_H(\bar{\kappa},\zeta',s) + \tilde{n}_T(\bar{\kappa},\zeta',s)], \tag{47}$$

$$\phi_b(\bar{\kappa},\zeta,s) = \int_\zeta^{Z/L_H} d\zeta' e^{-L_H/ct_0 s(\zeta'-\zeta)} \cos\left[\frac{\kappa^2}{2}(\zeta'-\zeta)\right] \times[\tilde{n}_H(\bar{\kappa},\zeta',s) + \tilde{n}_T(\bar{\kappa},\zeta',s)]. \tag{48}$$

Substitution of the result in Eq. (46) into the result in Eqs. (47) and (48) gives

$$\chi_b(\bar{\kappa},\zeta,s) = -2\int_\zeta^{Z/L_H} d\zeta' e^{-L_H/ct_0 s(\zeta'-\zeta)} \times\sin\left[\frac{\kappa^2}{2}(\zeta'-\zeta)\right]\frac{\tilde{\alpha}(\zeta')}{s - i\bar{\kappa}\cdot\tilde{\mathbf{v}}(\zeta')}\chi_H(\bar{\kappa},\zeta',s) + \int_\zeta^{Z/L_H} d\zeta' e^{-L_H/ct_0 s(\zeta'-\zeta)} \times\sin\left[\frac{\kappa^2}{2}(\zeta'-\zeta)\right]\tilde{n}_T(\bar{\kappa},\zeta',s), \tag{49}$$

$$\phi_b(\bar{\kappa},\zeta,s) = -2\int_\zeta^{Z/L_H} d\zeta' e^{-L_H/ct_0 s(\zeta'-\zeta)} \times\cos\left[\frac{\kappa^2}{2}(\zeta'-\zeta)\right]\frac{\tilde{\alpha}(\zeta')}{s - i\bar{\kappa}\cdot\tilde{\mathbf{v}}(\zeta')}\chi_H(\bar{\kappa},\zeta',s) + \int_\zeta^{Z/L_H} d\zeta' e^{-L_H/ct_0 s(\zeta'-\zeta)} \times\cos\left[\frac{\kappa^2}{2}(\zeta'-\zeta)\right]\tilde{n}_T(\bar{\kappa},\zeta',s). \tag{50}$$

Next, note that the equations for the propagation of the high-energy laser beam can also be solved easily:

$$\chi_H(\bar{\kappa},\zeta,s) = e^{-L_H/ct_0 s\zeta}\cos\left(\frac{\kappa^2}{2}\zeta\right)\chi_H(\kappa,\zeta=0,s) + e^{-L_H/ct_0 s\zeta}\sin\left(\frac{\kappa^2}{2}\zeta\right)\phi_H(\kappa,\zeta=0,s) + \int_0^\zeta d\zeta' e^{-L_H/ct_0 s(\zeta-\zeta')}\sin[(\kappa^2/2)(\zeta-\zeta')] \times[\tilde{n}_H(\bar{\kappa},\zeta',s) + \tilde{n}_T(\bar{\kappa},\zeta',s)]. \tag{51}$$

$$\phi_H(\bar{\kappa},\zeta,s) = e^{-L_H/ct_0 s\zeta}\cos\left(\frac{\kappa^2}{2}\zeta\right)\phi_H(\kappa,\zeta=0,s) - e^{-L_H/ct_0 s\zeta}\sin\left(\frac{\kappa^2}{2}\zeta\right)\chi_H(\kappa,\zeta=0,s) + \int_0^\zeta d\zeta' e^{-L_H/ct_0 s(\zeta-\zeta')}\cos\left[\frac{\kappa^2}{2}(\zeta-\zeta')\right] \times[\tilde{n}_H(\bar{\kappa},\zeta',s) + \tilde{n}_T(\bar{\kappa},\zeta',s)]. \tag{52}$$

The reader will note that the boundary condition at $\zeta=0$ can be applied easily by use of the Laplace transform convolution theorem, and the solution for $\tilde{n}_H(\bar{\kappa},\zeta,s)$ in Eq. (46) can be used as well to obtain

$$\chi_H(\bar{\kappa},\zeta,s) = e^{-L_H/ct_0 s\zeta}\cos\left(\frac{\kappa^2}{2}\zeta\right)A(s)\chi_b(\kappa,\zeta=0,s) + e^{-L_H/ct_0 s\zeta}\sin\left(\frac{\kappa^2}{2}\zeta\right)P(s)\phi_b(\kappa,\zeta=0,s) - 2\times\int_0^\zeta d\zeta' e^{-L_H/ct_0 s(\zeta-\zeta')} \times\sin\left[\frac{\kappa^2}{2}(\zeta-\zeta')\right]\frac{\tilde{\alpha}(\zeta')}{s - i\bar{\kappa}\cdot\tilde{\mathbf{v}}(\zeta')}\chi_H(\bar{\kappa},\zeta',s) + \int_0^\zeta d\zeta' e^{-L_H/ct_0 s(\zeta-\zeta')}\sin\left[\frac{\kappa^2}{2}(\zeta-\zeta')\right]\tilde{n}_T(\bar{\kappa},\zeta',s), \tag{53}$$

$$\phi_H(\bar{\kappa},\zeta,s) = e^{-L_H/ct_0 s\zeta}\cos\left(\frac{\kappa^2}{2}\zeta\right)P(s)\phi_b(\kappa,\zeta=0,s) - e^{-L_H/ct_0 s\zeta}\sin\left(\frac{\kappa^2}{2}\zeta\right)A(s)\chi_b(\kappa,\zeta=0,s) - 2\times\int_0^\zeta d\zeta' e^{-L_H/ct_0 s(\zeta-\zeta')} \times\cos\left[\frac{\kappa^2}{2}(\zeta-\zeta')\right]\frac{\tilde{\alpha}(\zeta')}{s - i\bar{\kappa}\cdot\tilde{\mathbf{v}}(\zeta)}\chi_H(\bar{\kappa},\zeta',s) + \int_0^\zeta d\zeta' e^{-L_H/ct_0 s(\zeta-\zeta')}\cos\left[\frac{\kappa^2}{2}(\zeta-\zeta')\right]\tilde{n}_T(\bar{\kappa},\zeta',s). \tag{54}$$

The final step is to substitute the expression for the the beacon beam into Eqs. (53) and (54) to obtain

$$\chi_H(\bar{\kappa},\zeta,s) = -2A(s)\int_0^{Z/L_H} d\zeta' e^{-L_H/ct_0 s(\zeta+\zeta')}\cos\left(\frac{\kappa^2}{2}\zeta\right)\sin\left(\frac{\kappa^2}{2}\zeta'\right)\frac{\tilde{\alpha}(\zeta')}{s-i\bar{\kappa}\cdot\tilde{\mathbf{v}}(\zeta')}\chi_H(\bar{\kappa},\zeta',s) - 2P(s)\int_0^{Z/L_H} d\zeta' e^{-L_H/ct_0 s(\zeta+\zeta')}$$
$$\times\sin\left(\frac{\kappa^2}{2}\zeta\right)\cos\left(\frac{\kappa^2}{2}\zeta'\right)\frac{\tilde{\alpha}(\zeta')}{s-i\bar{\kappa}\cdot\tilde{\mathbf{v}}(\zeta')}\chi_H(\bar{\kappa},\zeta',s) - 2\int_0^{\zeta} d\zeta' e^{-L_H/ct_0 s(\zeta-\zeta')}\sin\left[\frac{\kappa^2}{2}(\zeta-\zeta')\right]\frac{\tilde{\alpha}(\zeta')}{s-i\bar{\kappa}\cdot\tilde{\mathbf{v}}(\zeta')}\chi_H(\bar{\kappa},\zeta',s)$$
$$+A(s)\int_0^{Z/L_H} d\zeta' e^{-L_H/ct_0 s(\zeta+\zeta')}\cos\left(\frac{\kappa^2}{2}\zeta\right)\sin\left(\frac{\kappa^2}{2}\zeta'\right)\tilde{n}_T(\bar{\kappa},\zeta',s) + P(s)\int_0^{Z/L_H} d\zeta' e^{-L_H/ct_0 s(\zeta+\zeta')}$$
$$\times\sin\left(\frac{\kappa^2}{2}\zeta\right)\cos\left(\frac{\kappa^2}{2}\zeta'\right)\tilde{n}_T(\bar{\kappa},\zeta',s) + \int_0^{\zeta} d\zeta' e^{-L_H/ct_0 s(\zeta-\zeta')}\sin\left[\frac{\kappa^2}{2}(\zeta-\zeta')\right]\tilde{n}_T(\bar{\kappa},\zeta',s), \tag{55}$$

$$\phi_H(\bar{\kappa},\zeta,s) = -2P(s)\int_0^{Z/L_H} d\zeta' e^{-L_H/ct_0 s(\zeta'+\zeta)}\cos\left(\frac{\kappa^2}{2}\zeta\right)\cos\left(\frac{\kappa^2}{2}\zeta'\right)\frac{\tilde{\alpha}(\zeta')}{s-i\bar{\kappa}\cdot\tilde{\mathbf{v}}(\zeta')}\chi_H(\bar{\kappa},\zeta',s) + 2A(s)\int_0^{Z/L_H} d\zeta' e^{-L_H/ct_0 s(\zeta'+\zeta)}$$
$$\times\sin\left(\frac{\kappa^2}{2}\zeta\right)\sin\left(\frac{\kappa^2}{2}\zeta'\right)\frac{\tilde{\alpha}(\zeta')}{s-i\bar{\kappa}\cdot\tilde{\mathbf{v}}(\zeta')}\chi_H(\bar{\kappa},\zeta',s) - 2\int_0^{\zeta} d\zeta' e^{-L_H/ct_0 s(\zeta-\zeta')}\cos\left[\frac{\kappa^2}{2}(\zeta-\zeta')\right]\frac{\tilde{\alpha}(\zeta')}{s-i\bar{\kappa}\cdot\tilde{\mathbf{v}}(\zeta')}\chi_H(\bar{\kappa},\zeta',s)$$
$$+P(s)\int_0^{Z/L_H} d\zeta' e^{-L_H/ct_0 s(\zeta'+\zeta)}\cos\left(\frac{\kappa^2}{2}\zeta\right)\cos\left(\frac{\kappa^2}{2}\zeta'\right)\tilde{n}_T(\bar{\kappa},\zeta',s) - A(s)\int_0^{Z/L_H} d\zeta' e^{-L_H/ct_0 s(\zeta'+\zeta)}\sin\left(\frac{\kappa^2}{2}\zeta\right)$$
$$\times\sin\left(\frac{\kappa^2}{2}\zeta'\right)\tilde{n}_T(\bar{\kappa},\zeta',s) + \int_0^{\zeta} d\zeta' e^{-L_H/ct_0 s(\zeta-\zeta')}\cos\left[\frac{\kappa^2}{2}(\zeta-\zeta')\right]\tilde{n}_T(\bar{\kappa},\zeta',s). \tag{56}$$

Two points are immediately apparent from Eqs. (55) and (56). As expected, if $A(s)=1$ and $P(s)=-1$, and if the time of flight is neglected ($c\to\infty$), then at $\zeta=Z/L_H$, the right-hand side of both equations collapses to a Volterra integral operator. Because the integral over ζ' is Volterra, bounded solutions exist for all values of ζ, indicating stability of full-wave conjugation. This tells us that full-wave conjugation certainly has potential to compensate simultaneously for the effects of thermal blooming and turbulence. The second point of note is that Eq. (56) is explicitly determined by the solution of Eq. (55), and thus for purposes of consideration of existence of solutions of the linearized TBC equations, it is necessary to consider only Eq. (56).

Next, similar to the analysis approach adopted by Fried and Szeto [14], we consider the substitution of the heating-induced fluctuation in a local reference frame,

$$\chi_H(\bar{\kappa},\zeta,\tau) = \chi_H(\bar{\kappa},\zeta,\tau)e^{i\bar{\kappa}\cdot\tilde{\mathbf{v}}(\zeta')\tau}. \tag{57}$$

This substitution allows us to write the following equation which exposes the requirements for solutions for $\chi_H(\bar{\rho},\zeta,\tau)$ to exist. This equation is referred to as the amplitude perturbation integral (API) equation:

$$\chi_H(\bar{\kappa},\zeta,\tau) - \mathcal{M}[\chi_H(\bar{\kappa},\zeta,\tau)] = \tilde{\chi}_H(\bar{\kappa},\zeta,\tau), \tag{58}$$

$$\tilde{\chi}_H(\bar{\kappa},\zeta,\tau) = e^{-i\bar{\kappa}\cdot\tilde{\mathbf{v}}(\zeta')\tau}\mathcal{L}^{-1}(\mathcal{M}_0\{\mathcal{L}[\tilde{n}_T(\bar{\kappa},\zeta,\tau)]\}), \tag{59}$$

where $\mathcal{L}$ is the Laplace transform, and

$$\mathcal{M}[f(\bar{\kappa},\zeta,\tau)] = -2\int_0^{Z/L_H} d\zeta'\tilde{\alpha}(\zeta')\cos\left(\frac{\kappa^2}{2}\zeta\right)\sin\left(\frac{\kappa^2}{2}\zeta'\right)\int_0^{\tau} d\tau' a(\tau-\tau')\int_0^{\tau'-L_H/ct_0(\zeta+\zeta')} d\tau'' e^{i\bar{\kappa}\cdot\tilde{\mathbf{v}}(\zeta')\tau'-i\bar{\kappa}\cdot\tilde{\mathbf{v}}(\zeta)\tau-i\bar{\kappa}\cdot\tilde{\mathbf{v}}(\zeta')L_H/ct_0(\zeta+\zeta')}f(\bar{\kappa},\zeta',\tau'')$$
$$-2\int_0^{Z/L_H} d\zeta'\tilde{\alpha}(\zeta')\sin\left(\frac{\kappa^2}{2}\zeta\right)\cos\left(\frac{\kappa^2}{2}\zeta'\right)\int_0^{\tau} d\tau' p(\tau-\tau')\int_0^{\tau'-L_H/ct_0(\zeta+\zeta')} d\tau'' e^{i\bar{\kappa}\cdot\tilde{\mathbf{v}}(\zeta')\tau'-i\bar{\kappa}\cdot\tilde{\mathbf{v}}(\zeta)\tau-i\bar{\kappa}\cdot\tilde{\mathbf{v}}(\zeta')L_H/ct_0(\zeta+\zeta')}f(\bar{\kappa},\zeta',\tau'')$$
$$-2\int_0^{\zeta} d\zeta'\tilde{\alpha}(\zeta')\sin\left[\frac{\kappa^2}{2}(\zeta-\zeta')\right]\int_0^{\tau-L_H/ct_0(\zeta-\zeta')} d\tau' e^{i\bar{\kappa}\cdot[\tilde{\mathbf{v}}(\zeta')-\tilde{\mathbf{v}}(\zeta)]\tau-i\bar{\kappa}\cdot\tilde{\mathbf{v}}(\zeta')L_H/ct_0(\zeta-\zeta')}f(\bar{\kappa},\zeta',\tau'), \tag{60}$$

$$\mathcal{M}_0[f(\bar{\kappa},\zeta,s)] = A(s)\int_0^{Z/L_H} d\zeta' e^{-L_H/ct_0 s(\zeta+\zeta')}\cos\left(\frac{\kappa^2}{2}\zeta\right)\sin\left(\frac{\kappa^2}{2}\zeta'\right)f(\bar{\kappa},\zeta',s) + P(s)\int_0^{Z/L_H} d\zeta' e^{-L_H/ct_0 s(\zeta+\zeta')}\sin\left(\frac{\kappa^2}{2}\zeta\right)$$
$$\times\cos\left(\frac{\kappa^2}{2}\zeta'\right)f(\bar{\kappa},\zeta',s) + \int_0^{\zeta} d\zeta' e^{-L_H/ct_0 s(\zeta-\zeta')}\sin\left[\frac{\kappa^2}{2}(\zeta-\zeta')\right]f(\bar{\kappa},\zeta',s). \quad (61)$$

B. Treatment of the Effects of Microscale Random Wind Shear

The effects of microscale random wind shear are introduced by writing the wind velocity along the path as the mean along the path plus a structured and unstructured (random) perturbation $\tilde{\mathbf{v}}(\zeta)=\tilde{\mathbf{v}}_0+\tilde{\mathbf{v}}_1(\zeta)+\delta\tilde{\mathbf{v}}(\zeta)$. The variable $\tilde{\mathbf{v}}_0$ is defined as the mean wind velocity along the path $\tilde{\mathbf{v}}_0=1/Z/L_H\int_0^{Z/L_H}d\zeta\tilde{\mathbf{v}}(\zeta)$. The variable $\tilde{\mathbf{v}}_1(\zeta)$ is a structured deviation from the mean along the path. This would be a measured average wind profile along the propagation, ostensibly a smoothly varying fit to some coarse set of data for values of the mean wind velocity along the path. The variable $\delta\tilde{\mathbf{v}}(\zeta)$ is the random, unstructured variations of the wind velocity along the path. This contribution is what will provide the desired PCI stabilizing effect. With this description of the wind along the path, one can write

$$\exp\{ia\bar{\kappa}\cdot\tilde{\mathbf{v}}(\zeta)\} = \exp\{ia2\bar{\kappa}\cdot\tilde{\mathbf{v}}_0\} \times\exp\{ia\bar{\kappa}\cdot\tilde{\mathbf{v}}_1(\zeta)\}\exp\{ia\bar{\kappa}\cdot\delta\tilde{\mathbf{v}}(\zeta)\}. \quad (62)$$

There is some difficulty associated with treatment of the microscale random wind shear because the statistics of the random fluctuations are nonstationary. We adopt an approximate approach similar to that of Sasiela [22] and treat the statistics as being stationary locally for the purpose of developing the spectrum of fluctuations, but nonstationary over the entire path. The structure function of perturbations for each axis is then found to be

$$D_{\delta\tilde{v}}(\zeta_1,\zeta_2) = \frac{4}{v_0^2}\int_0^{\infty} d\kappa_z[1-\cos(2\pi\kappa_z|\zeta_1-\zeta_2|)] \times\Psi[\kappa_z/L_H,(\zeta_1+\zeta_2)L_H/2], \quad (63)$$

with the spectrum of perturbations being given by

$$\Psi(\kappa_z,z) = 0.00969\frac{\pi}{2}\frac{\Gamma\left(\frac{5}{6}\right)}{\Gamma\left(\frac{11}{6}\right)}C_v^2(z)[\kappa_z^2+1/L_0^2(z)]^{-5/6} \times\exp\left[-\kappa^2\ell_0^2(z)\frac{4\pi^2}{5.91^2}\right], \quad (64)$$

where ℓ_0 and L_0 are the inner and outer scale, respectively. Note that we assume that the two components of $\delta\tilde{\mathbf{v}}(\zeta)$ are uncorrelated and have the same spectrum. The velocity structure constant $C_v^2(z)$ is related to the refractive index structure constant $C_n^2(z)$ in a complicated manner. The length scales for velocity fluctuations are a function of the velocity structure constant along the path and in turn related to the length scales for the refractive index structure constant. The measurement data necessary to make the appropriate conversion generally is not readily available, and we suggest that velocity structure constant measurements in conjunction with refractive index structure constant measurements would be ideal.

In addition to the structure function of wind velocity perturbations, the variance of the microscale random wind shear at a location ζ over an interval $[\zeta_1,\zeta_2]$ is useful. This quantity is given by

$$V(\zeta,\zeta_1,\zeta_2) = \left\langle\left[\delta\tilde{v}(\zeta) - \frac{1}{\zeta_2-\zeta_1}\int_{\zeta_1}^{\zeta_2} d\zeta'\,\delta\tilde{v}(\zeta')\right]^2\right\rangle \quad (65)$$

$$= \frac{1}{\zeta_2-\zeta_1}\int_{\zeta_1}^{\zeta_2} d\zeta' D_{\delta\tilde{v}}(\zeta,\zeta') - \frac{1/2}{(\zeta_2-\zeta_1)^2}\int_{\zeta_1}^{\zeta_2} d\zeta'\int_{\zeta_1}^{\zeta_2} d\zeta'' D_{\delta\tilde{v}}(\zeta',\zeta''). \quad (66)$$

An additional quantity of interest that will be examined is the wind shear variance averaged over an interval,

$$\bar{V}(\zeta_1,\zeta_2) = \frac{1}{\zeta_2-\zeta_2}\int_{\zeta_1}^{\zeta_2} d\zeta V(\zeta,\zeta_1,\zeta_2). \quad (67)$$

Finally, the special case of an infinite outer scale and zero inner scale provides a form that will be utilized further in the analysis. In this case, it is of value to define the normalized quantity $\tilde{V}(Z)$ as

$$\tilde{V}(Z) = \int_0^1 d\zeta\int_0^1 d\zeta' C_{\tilde{v}}^2\left(\frac{\zeta+\zeta'}{2}\frac{Z}{L_H}\right)|\zeta-\zeta'|^{2/3} - \frac{1}{2}\int_0^1 d\zeta'\int_0^1 d\zeta'' C_{\tilde{v}}^2\left(\frac{\zeta'+\zeta''}{2}\frac{Z}{L_H}\right)|\zeta'-\zeta''|^{2/3}, \quad (68)$$

$$C_V^2 = \frac{1}{Z}\int_0^Z dz C_v^2(z), \quad (69)$$

and note that $\bar{V}(0,Z)=C_V^2/v_0^2/Z^{2/3}\tilde{V}(Z)$ and $C_v^2(z)=C_V^2C_{\tilde{v}}^2(\zeta)$.

The structure function representation of microscale random wind shear will be used to develop the most general expressions describing mitigation of compensation instabilities, while the forms of the variance of microscale random wind shear will be used to compute approximate

quantities that more readily provide intuition into the key parameters that affect stability of the compensation systems of interest.

5. EXAMINATION OF PARTICULAR CONFIGURATIONS FOR COMPENSATED THERMAL BLOOMING

In this section, expressions that ensure the existence of bounded solutions to the API equation are developed:

$$\chi_H(\bar{\kappa},\zeta,\tau) - \mathcal{M}[\chi_H(\bar{\kappa},\zeta,\tau)] = \tilde{\chi}_{\mathcal{H}}(\bar{\kappa},\zeta,\tau). \tag{70}$$

In this paper, the term stability is taken to imply that bounded solutions to the API equation exist for all time. There are two general approaches for handling the treatment of the existence of bounded solutions of Eq. (70) that are illustrated in this section. Both rely on the use of the contraction mapping theorem. The first case, phase compensation, is detailed in subsection 5.A. The second case, full-wave compensation with time of flight delay, is described in subsection 5.B.

A. Instantaneous Phase-Only Compensation; No Time of Flight

In the first case considered, we quantify the ability of random microscale wind shear to mitigate PCI. This section is organized to lead the reader through problem setup including introduction of the concept of the averaged API equation, to outlining the requirements for stability of the system (these requirements are derived in Appendix A), and then to consider reduction of the resultant requirements to fundamental parameters that are similar to scaling laws that characterize the mitigation of phase compensation instability by microscale random wind shear along the propagation path.

The reader should note that phase compensation is not immune to the destabilizing effect of time of flight. However, the impact of time of flight on phase compensation in terms of stability is small relative to the impact of classical phase compensation instability. This is the justification for our neglecting the impact of time of flight in the current work.

The problem of instantaneous phase compensation without time of flight is described by setting the control filters to $a(\tau)=0$ and $p(\tau)=-\delta(\tau)$ and letting $(c\to\infty)$. Making these definitions the operator $\mathcal{M}$ is given by

$$\begin{aligned}\mathcal{M}[f(\bar{\kappa},\zeta,\tau)] = 2\int_0^{\zeta} \mathrm{d}\zeta' \tilde{\alpha}(\zeta')\cos\left(\frac{\kappa^2}{2}\zeta\right)\sin\left(\frac{\kappa^2}{2}\zeta'\right)e^{i\bar{\kappa}\cdot[\tilde{\mathbf{v}}(\zeta')-\tilde{\mathbf{v}}(\zeta)]\tau}\\ \times\int_0^{\tau}\mathrm{d}\tau' f(\bar{\kappa},\zeta',\tau') + 2\int_{\zeta}^{Z/L_H}\mathrm{d}\zeta'\tilde{\alpha}(\zeta')\sin\left(\frac{\kappa^2}{2}\zeta\right)\\ \times\cos\left(\frac{\kappa^2}{2}\zeta'\right)e^{i\bar{\kappa}\cdot[\tilde{\mathbf{v}}(\zeta')-\tilde{\mathbf{v}}(\zeta)]\tau}\int_0^{\tau}\mathrm{d}\tau' f(\bar{\kappa},\zeta',\tau').\end{aligned} \tag{71}$$

This equation is not readily treated by analytic procedures. However, it has been arranged in a form that can be analyzed under the assumption that analysis of the ensemble average of the integral equation provides a sound basis for analysis of the general system. This brings the discussion to the concept of the averaged API equation. Consider the ensemble average of the operator $\mathcal{M}$ to produce the average operator $\bar{\mathcal{M}}$, where the ensemble averaging is over the statistics of microscale random wind shear. If we ensemble-average the expression for $\mathcal{M}$ in Eq. (71) we obtain

$$\begin{aligned}\bar{\mathcal{M}}[f(\bar{\kappa},\zeta,\tau)] = 2\int_0^{\zeta}\mathrm{d}\zeta'\tilde{\alpha}(\zeta')\cos\left(\frac{\kappa^2}{2}\zeta\right)\\ \times\sin\left(\frac{\kappa^2}{2}\zeta'\right)e^{-1/2\kappa^2 D_{\delta\tilde{v}}(\zeta,\zeta')\tau^2}\\ \times\int_0^{\tau}\mathrm{d}\tau' f(\bar{\kappa},\zeta',\tau') + 2\int_{\zeta}^{Z/L_H}\mathrm{d}\zeta'\tilde{\alpha}(\zeta')\\ \times\sin\left(\frac{\kappa^2}{2}\zeta\right)\cos\left(\frac{\kappa^2}{2}\zeta'\right)e^{-1/2\kappa^2 D_{\delta\tilde{v}}(\zeta,\zeta')\tau^2}\\ \times\int_0^{\tau}\mathrm{d}\tau' f(\bar{\kappa},\zeta',\tau').\end{aligned} \tag{72}$$

Note that we have assumed here that the smooth variations in the profile are insufficient to cause a significant mitigation of PCI and instead focused only on the microscale wind shear. The reader should also note that although we do not plan to study the impact of smoothly varying wind velocity fluctuations in this paper, there is nothing preventing the joint treatment of these fluctuations using the structure function formalism.

The reader should further note that we readily accept that a solution of the averaged API equation

$$\chi_H(\bar{\kappa},\zeta,\tau) - \bar{\mathcal{M}}[\chi_H(\bar{\kappa},\zeta,\tau)] = \tilde{\chi}_H(\bar{\kappa},\zeta,\tau) \tag{73}$$

is not equivalent to ensemble averaging of the formal Neumann series solution of the API equation

$$\chi_H(\bar{\kappa},\zeta,\tau) = \sum_{k=0}^{\infty}\mathcal{M}^k\{[\tilde{\chi}_H(\bar{\kappa},\zeta,\tau)]\}. \tag{74}$$

However, we expect that inclusion of the higher-order correlations that would arise in ensemble averaging of the Neumann series solution would only lead to further amelioration of the effects of PCI; that is, consideration of the averaged API Eq. (73) is suspected to be conservative.

Formal consideration of existence of the solutions of the API or averaged API equation by means of an elementary application of the contraction mapping theorem is included in Appendix A. The analysis in Appendix A defines the integral operator

$$T_{PO}[\chi_H(\bar{\kappa},\zeta,\tau)] = \mathcal{M}[\chi_H(\bar{\kappa},\zeta,\tau)] + \tilde{\chi}_{\mathcal{H}}(\bar{\kappa},\zeta,\tau) \tag{75}$$

and consider solutions to the equation

$$T_{PO}[\chi_H(\bar{\kappa},\zeta,\tau)] = \chi_H(\bar{\kappa},\zeta,\tau), \tag{76}$$

where $\zeta\in[0,Z/L_H]$ and $\tau\in[0,T]$. Bounded solutions for all $T\in[0,\infty]$ are desired. Define the space of interest X to be the space of continuous functions defined on ζ and τ, $X=\mathcal{C}([0,Z/L_H]\times[0,T])$. Under the assumption that one can compute a bound θ_{PO} such that $\|\mathcal{M}\|\leq\theta_{PO}<1$ for all ζ

and for all T, we show in Appendix A that solutions exist and are bounded using an elementary application of the contraction mapping theorem.

The next step in the analysis is computation of the bound θ_{PO} on the norm of the average operator $\bar{\mathcal{M}}$. The value of θ_{PO} as a function of κ can be bounded by

$$\theta_{PO}(\kappa) \leq \sup_{\substack{\zeta\in[0,Z/L_H]\\ \tau\in(0,\infty)}} 2\tau\int_0^{\zeta} d\zeta'\tilde{\alpha}(\zeta') \times\left|\cos\left(\frac{\kappa^2}{2}\zeta\right)\sin\left(\frac{\kappa^2}{2}\zeta'\right)\right| e^{-1/2\kappa^2 D_{\delta\bar{v}}(\zeta,\zeta')\tau^2} + 2\tau\int_{\zeta}^{Z/L_H} d\zeta'\tilde{\alpha}(\zeta') \times\left|\sin\left(\frac{\kappa^2}{2}\zeta\right)\cos\left(\frac{\kappa^2}{2}\zeta'\right)\right| e^{-1/2\kappa^2 D_{\delta\bar{v}}(\zeta,\zeta')\tau^2}. \quad (77)$$

There are several observations of note regarding Eq. (77). The bound on the norm of $\bar{\mathcal{M}}$ has a linear growth component that is mitigated by the exponential decay term associated with microscale random wind shear. At some value of τ these effects come into balance, defining the maximum gain and the associated stability bound. Computation of Eq. (77) is necessarily restricted to direct numerical evaluation, likely most easily computed using a search over $\zeta\in[0,Z/L_H]$ and over $\tau\in[0,\infty)$. Note that it is in general impractical to search over an arbitrary bound in τ. Based on the analysis to follow, it is safe to search over the regime $\tau\in[0,2/\kappa\sqrt{2\bar{V}(0,Z/L_H)}]$. The approximate upper bound was derived by use of the Marechal approximation, which enables us to develop expressions that are analogous to scaling laws for propagation through turbulence.

A small variation on the Marechal approximation provides the relationship

$$\frac{\int_{\zeta_1}^{\zeta_2} d\zeta' W(\zeta,\zeta') e^{-1/2\kappa^2 D_{\delta\bar{v}}(\zeta,\zeta')\tau^2}}{\int_{\zeta_1}^{\zeta_2} d\zeta' W(\zeta,\zeta')} \approx \exp[-w_a\kappa^2\tau^2 V(\zeta,\zeta_1,\zeta_2)], \quad (78)$$

where $w_a=1/\sqrt{2}$ for κ small and $w_a=1$ for κ large. The modification to the Marechal approximation is used to obtain better agreement for the small asymptote for κ. This reduction in the impact of fluctuations was found to be a better approximation due to the reduced independence of fluctuations at low frequencies. Using the modified Marechal approximation we can write the following approximate form for a bound on $\theta_{PO}(\kappa)$:

$$\theta_{PO}(\kappa) \leq \max_{\tau\in(0,\infty)} 2\tau e^{-w_a\kappa^2\tau^2\bar{V}(0,Z/L_H)} \max_{\zeta\in[0,Z/L_H]} I_0(\zeta,\kappa) \quad (79)$$

$$= \frac{1}{\kappa}\frac{2^{1/2}e^{-1/2}}{w_a^{1/2}\sqrt{\bar{V}(0,Z/L_H)}} \max_{\zeta\in[0,Z/L_H]} I_0(\zeta,\kappa), \quad (80)$$

$$I_0(\zeta,\kappa) = \int_0^{\zeta} d\zeta'\tilde{\alpha}(\zeta')\left|\cos\left(\frac{\kappa^2}{2}\zeta\right)\sin\left(\frac{\kappa^2}{2}\zeta'\right)\right| + \int_{\zeta}^{Z/L_H} d\zeta'\tilde{\alpha}(\zeta')\left|\sin\left(\frac{\kappa^2}{2}\zeta\right)\cos\left(\frac{\kappa^2}{2}\zeta'\right)\right|, \quad (81)$$

where we utilized the fact that the maximum value is achieved for $\tau=1/\kappa 2^{1/2}w_a^{1/2}\sqrt{\bar{V}(0,Z/L_H)}$.

In general, computation of $I_0(\zeta,\kappa)$ requires numerical evaluation. However, it is worth consideration of the asymptotic values for small and large κ. For small κ we write

$$\lim_{\kappa\to 0} I_0(\zeta,\kappa) \approx \frac{\kappa^2}{2}\left[\int_0^{\zeta} d\zeta'\tilde{\alpha}(\zeta')\zeta' + \zeta\int_{\zeta}^{Z/L_H} d\zeta'\tilde{\alpha}(\zeta')\right]. \quad (82)$$

The maximum value of $I_0(\zeta,\kappa)$ for small values of κ is achieved for $\zeta=Z/L_H$. This is straightforward to show using the calculus of variations (use Leibniz formula). For large κ we write

$$\lim_{\kappa\to\infty} I_0(\zeta,\kappa) \approx \frac{2}{\pi}\int_0^{Z/L_H} d\zeta'\tilde{\alpha}(\zeta') = \frac{2}{\pi}\frac{Z}{L_H}. \quad (83)$$

Applying these values to $\theta_{PO}(\kappa)$ asymptotic values can be found for small κ [recall that the maximum value of $I_0(\zeta,\kappa)$ is achieved for $\zeta=Z/L_H$],

$$\lim_{\kappa\to 0} \theta_{PO}(\kappa) \leq \frac{\kappa}{2}\frac{2^{1/2}e^{-1/2}}{w_a^{1/2}\sqrt{\bar{V}(0,Z/L_H)}}\int_0^{Z/L_H} d\zeta'\tilde{\alpha}(\zeta')\zeta', \quad (84)$$

and large κ,

$$\lim_{\kappa\to\infty} \theta_{PO}(\kappa) \leq \frac{1}{\kappa}\frac{2}{\pi}\frac{Z}{L_H}\frac{2^{1/2}e^{-1/2}}{w_a^{1/2}\sqrt{\bar{V}(0,Z/L_H)}}. \quad (85)$$

At this point, the generalized API parameters are introduced. The API parameters are similar to the WISP parameter introduced by Fried and Szeto [14].

First, consider the API parameters $\eta_1(\kappa)$ and $\eta_{-1}(\kappa)$, valid for small and large κ, respectively:

$$\eta_1(\kappa) = \left[\frac{v_0 2^{1/2}e^{-1/2}}{\sqrt{C_V^2 Z^{2/3}\tilde{V}(Z/L_H)}}\right] w_1^{-1/2}2^{-1}\kappa\frac{Z^2}{L_H^2}\mu_{\tilde{\alpha},1}, \quad (86)$$

$$\eta_{-1}(\kappa) = \left[\frac{v_0 2^{1/2}e^{-1/2}}{\sqrt{C_V^2 Z^{2/3}\tilde{V}(Z/L_H)}}\right] w_{-1}^{-1/2}2^{1}\frac{1}{\pi}\frac{1}{\kappa}\frac{Z}{L_H}, \quad (87)$$

$$\mu_{\tilde{\alpha},1} = \int_0^1 d\zeta'\tilde{\alpha}(\zeta' Z/L_H)\zeta', \quad (88)$$

where $w_1=1/\sqrt{2}$ and $w_{-1}=1$. Noting that there exists a crossing point where $\eta_1(\kappa)=\eta_{-1}(\kappa)$, we can define the parameter η_0 and the crossing frequency κ_0 with

$$\eta_0 = \left[\frac{v_0 2^{1/2}e^{-1/2}}{\sqrt{C_V^2 Z^{2/3}\tilde{V}(Z/L_H)}}\right] w_1^{-1/4}w_{-1}^{-1/4}\frac{\mu_{\tilde{\alpha},1}^{1/2}Z^{3/2}}{\pi^{1/2}L_H^{3/2}}, \quad (89)$$

$$\kappa_0 = 2\sqrt{\frac{L_H}{\pi Z \mu_{\tilde{\alpha},1}}}\left(\frac{w_1}{w_{-1}}\right)^{1/4}. \tag{90}$$

The API parameters noted above are characterized by the generalized API parameter

$$\eta_N(\kappa) = \left[\frac{v_0 2^{1/2} e^{-1/2}}{\sqrt{C_V^2 Z^{2/3}\tilde{V}(Z/L_H)}}\right] w_1^{-1/4} w_{-1}^{-1/4} \frac{\mu_{\tilde{\alpha},1}^{1/2} Z^{3/2}}{\pi^{1/2} L_H^{3/2}} \kappa^N \left(\frac{w_{-1}}{w_1}\right)^{N/4} \times \left[\frac{\pi Z \mu_{\tilde{\alpha},1}}{4L_H}\right]^{N/2} \tag{91}$$

$$= \eta_0 \left(\frac{\kappa}{\kappa_0}\right)^N. \tag{92}$$

The API parameter η_0 is taken to be *the* API parameter as we will find it to appear in the scaling for full-wave conjugation with time of flight delay as well. If we substitute the expression for the length scale L_H, we find the following result, which clearly illustrates all of the desired and expected scaling relationships:

$$\eta_0 = \frac{2^{1/2} e^{-1/2} w_1^{-1/4} w_{-1}^{-1/4} \mu_{\tilde{\alpha},1}^{1/2}}{\pi^{1/2}} \left[\frac{v_0 Z^{3/2} \alpha_0 E_0^2 k_0^{1/2}}{\sqrt{C_V^2 Z^{2/3}\tilde{V}(Z/L_H)}}\right] \tag{93}$$

$$= 0.5277 \mu_{\tilde{\alpha},1}^{1/2} \left[\frac{v_0 Z^{3/2} \alpha_0 E_0^2 k_0^{1/2}}{\sqrt{C_V^2 Z^{2/3}\tilde{V}(Z/L_H)}}\right]. \tag{94}$$

There is significant utility to these expressions. In Fig. 1, curves are shown that represent maximum values of η_0 as a function of normalized spatial frequency to ensure existence of stable solutions. The curves are the value of η_0 for which $\theta_{PO}(\kappa)=1$ with results calculated using both an accurate numerical evaluation and the Marechal approximation ($w_a = w_1$ for this evaluation), the value of η_0 for which $\eta_{-1}=1$, and the value of η_0 for which $\eta_1=1$. It is assumed that $\tilde{\alpha}(\zeta)$ and $C_v^2(\zeta)$ are constant along the path

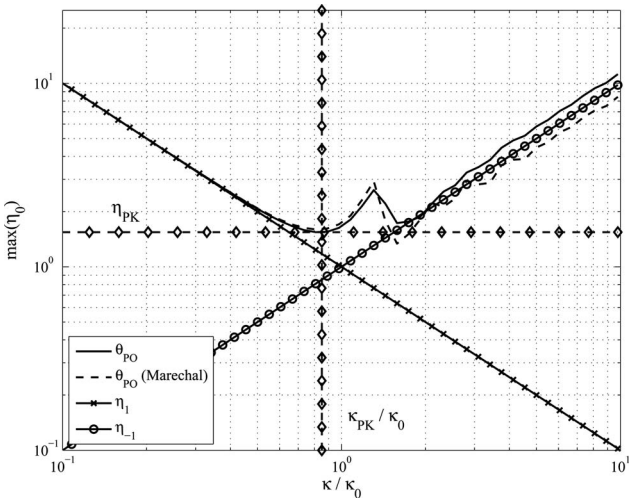

Fig. 1. Maximum value of the API parameter η_0 as a function of normalized spatial frequency κ/κ_0 to ensure stability for phase compensation. The figure provides the asymptotic bounds as well as the peak bound (marked with diamonds). The peak frequency is illustrated as well (marked with diamonds).

to generate this example. The approximate bounds that are computed using the generalized API parameters are tight, and we note that although the high-frequency bound is conservative at the highest frequencies, it is achieved at an intermediate frequency.

The physical intuition behind the nature of the curve is relatively straightforward. It is well known that PCI is a spatial-frequency-dependent phenomenon: compensation at low spatial frequencies is less prone to instability, thus describing the nature of the low frequency asymptote. As the spatial frequency for compensation increases, the API parameter becomes smaller, corresponding to an increased sensitivity to PCI (i.e., one could relate this to a maximum power level defining the onset of PCI). However, at some point with increasing spatial frequency, the mitigating effects of microscale wind shear begin to take hold, controlling the instability and leading to the asymptote corresponding to high spatial frequencies.

The reader will also note two dashed curves in Fig. 1 labeling the peak value of the stability bound η_{PK} and the corresponding frequency κ_{PK}. From the curve, one may think that the peak was computed from the bound $\theta_{PO}(\kappa)$. Rather, we considered the leading-order terms in the expression for $\theta_{PO}(\kappa)$ using the Marechal approximation, then, using calculus of variations, computed the value for the peak frequency

$$\kappa_{PK}^4 = \frac{1-\mu_{\tilde{\alpha},1}}{\frac{1}{4}+\frac{1}{8}\mu_{\tilde{\alpha},1}}\left(\frac{L_H}{Z}\right)^2. \tag{95}$$

Evaluating $\theta_{PO}(\kappa)$ at the peak frequency, we found

$$\eta_{PK} = \frac{1}{\kappa_{PK} w^{1/2}(\kappa_{PK})} \frac{v_0 2^{1/2} e^{-1/2}}{\sqrt{C_V^2 Z^{2/3}\tilde{V}(Z/L_H)}} \frac{Z}{L_H} \times \cos\left(\frac{\kappa^2}{2}\frac{Z}{L_H}\right) \mu_{\tilde{\alpha},S}\left(\frac{\kappa_{PK}^2}{2}\right), \tag{96}$$

$$\mu_{\tilde{\alpha},S}(a) = \int_0^1 d\zeta' \tilde{\alpha}\left(\zeta'\frac{Z}{L_H}\right) \sin\left(a\zeta'\frac{Z}{L_H}\right), \tag{97}$$

$$w(\kappa) = 2^{-1/2(1+\kappa^4/\kappa_0^4)}. \tag{98}$$

The expression for $w(\kappa)$ constitutes an intuitive "guess" at a function that gracefully transitions from $2^{-1/2}$ at $\kappa \to 0$, to $2^{-1/4}$ at $\kappa = \kappa_0$, and finally to 0 as $\kappa \to \infty$. The choice of the 4th power is simply due to the form determined for κ_{PK}.

The nature of the exact curve for the bound on η_0 is quite similar to the stability bound computed by Fried and Szeto [14]. This is not a surprise: Fried and Szeto defined the WISP parameter η_{WISP} as

$$\eta_{WISP} = \frac{Z^{3/2}\alpha_0 E_0^2 k_0^{1/2}}{2\sqrt{2\pi}\sqrt{C_V^2 Z^{2/3}\tilde{V}(Z/L_H)}}\left(\frac{L_0}{Z}\right)^{1/2}, \tag{99}$$

where

$$L_0 = Z\int_0^1 \mathrm{d}\zeta' \frac{\alpha(\zeta')}{\alpha(0)}. \tag{100}$$

Using this result we write

$$\eta_0 = 2.6457\mu_{\tilde{\alpha},1}^{1/2}\left(\frac{Z}{L_0}\right)^{1/2}\eta_{WISP}. \tag{101}$$

Here we find the reassuring result that the WISP parameter is proportional to the API parameter. The proportionality constants for the WISP and API parameter are slightly different moments of the turbulence profile. For a constant absorption profile, $\eta_0 = 1.3229\,\eta_{WISP}$. For a negative exponential absorption profile (corresponding to the simulation-based validation performed by Fried and Szeto), $\eta_0 = 1.6724\,\eta_{WISP}$. If we examine the ratio of η_0/η_{PK}, the value is 1.5438. In Fig. 6 of Fried and Szeto [14] a curve analogous to $\eta_{WISP}/\theta_{PO}(\kappa)$ is plotted and shown to have a minimum value of η_{WISP} very nearly 1.0, which would correspond to a minimum value of η_0 of 1.3229 for a constant profile and 1.6724 for a negative exponential absorption profile; thus our observed ratio for η_0/η_{PK} of 1.5438 is consistent with the equivalent values for η_{WISP}. Further, we note that the experimental data plotted in Fig. 6 of Fried and Szeto falls exactly on the stability boundary, whereas this same experimental point (which corresponds to a uniform absorption profile) would fall clearly above our stability boundary, suggesting that our parameterization using the integral equation technique captured by $\theta_{PO}(\kappa)$ may be more accurate [14]. The reader should note that repeating Fried and Szeto's analysis would be extremely difficult given the limited information describing the technique utilized. This is why we have taken an approximate route for comparison here (i.e., only by reference). There is some further difficulty in performing a direct comparison given that the calculations represented in Fig. 6 are for a negative exponential absorption profile, but the experimental results are for a uniform absorption profile.

Despite the caveats and difficulty in performing a direct comparison, we find the reasonably close agreement between our method and that of Fried and Szeto to be highly reassuring. The technique developed here is more transparent and more intuitive, and it leads to development of the fundamental parameters η_0 and κ_0.

Given that the parameters η_0, $\eta_1(\kappa)$, $\eta_{-1}(\kappa)$, and η_{PK} together form bounds for $\theta_{PO}(\kappa)$, and given the result that our stability bounds are comparable to those computed and validated by Fried and Szeto (particularly given that the trends associated with our results indicate that they may be more accurate), it is worth clearly documenting a procedure for evaluating the stability of a propagation scenario. We define this process in a list of steps:

1. Define a range of normalized spatial frequencies to be corrected $\kappa \in [l_f/D, l_f/l]$, where D is the aperture diameter, l is the actuator spacing, and recall $l_f = \sqrt{L_H/k_0}$ is the Fresnel zone size.
2. Compute η_0 for the propagation scenario, from which $\eta_1(\kappa)$ and $\eta_{-1}(\kappa)$ are then computed.
3. Compute η_{PK}.
4. If one of the following three conditions holds for all spatial frequencies $\kappa \in [l_f/D, l_f/l]$, then the system is stable: (a) $\eta_{PK} < 1$, (b) $\eta_1(\kappa) < 1$, or (c) $\eta_{-1}(\kappa) < 1$.

This approach is reasonably nonconservative, given the results in Fig. 1. Note that the condition in item 4 above inherently captures the scenario where $\kappa_{PK} > l_f/l$, but $\eta_{PK} > 1$. This may not be an uncommon scenario.

B. Instantaneous Full-Wave Compensation; Time of Flight Included

Having addressed the case of phase conjugation, attention is now turned to the potential instability in full-wave conjugation induced by laser time of flight. The control filters are set to $a(\tau) = \delta(\tau)$ and $p(\tau) = -\delta(\tau)$. The effects of time of flight are included. The same averaging procedure as for phase-only compensation is applied here. It will be convenient for this case to break up the averaged API operator for full-wave conjugation $\bar{\mathcal{M}}$ into two parts $\bar{\mathcal{M}} = \bar{\mathcal{K}} + \bar{\Delta}$ given by

$$\bar{\mathcal{K}}[f(\bar{\kappa},\zeta,\tau)] = 2\int_{\zeta}^{Z/L_H} \mathrm{d}\zeta' \tilde{\alpha}(\zeta')\sin\left[\frac{\kappa^2}{2}(\zeta-\zeta')\right] e^{-1/2\kappa^2 D_{\delta\bar{0}}(\zeta,\zeta')\tau^2} \times \int_0^{\tau} \mathrm{d}\tau' f(\bar{\kappa},\zeta',\tau'), \tag{102}$$

$$\bar{\Delta}[f(\bar{\kappa},\zeta,\tau)] = -2\int_{0}^{\zeta} \mathrm{d}\zeta' \tilde{\alpha}(\zeta')\sin\left[\frac{\kappa^2}{2}(\zeta-\zeta')\right] e^{-1/2\kappa^2 D_{\delta\bar{0}}(\zeta,\zeta')\tau^2} \times \int_{-\tau+L_H/ct_0(\zeta-\zeta')}^{-\tau+L_H/ct_0(\zeta+\zeta')} \mathrm{d}\tau' f(\bar{\kappa},\zeta',\tau'). \tag{103}$$

The reason for this approach is that although the sum of the two operators is not Volterra, treated separately they are both Volterra integral operators, and furthermore the norm of $\bar{\Delta}$ is controlled to be small because the speed of light is large, making the extent of the integration over τ' small (the reader should note that the fact that $\bar{\Delta}$ is Volterra is not required for our analysis; the fact that the norm of $\bar{\Delta}$ is small provides the required effect).

In Appendix B, we derive the requirements for existence of unique, bounded solutions on the space $X = C([0, Z/L_H]\times[0,T])$ on the averaged API equation for full-wave conjugation, $T_{FW}[\chi_H(\bar{\kappa},\zeta,\tau)] = \chi_H(\bar{\kappa},\zeta,\tau)$, where

$$T_{FW}[\chi_H(\bar{\kappa},\zeta,\tau)] = \bar{\mathcal{K}}[\chi_H(\bar{\kappa},\zeta,\tau)] + \bar{\Delta}[\chi_H(\bar{\kappa},\zeta,\tau)] + \tilde{\chi}_{\mathcal{H}}(\bar{\kappa},\zeta,\tau). \tag{104}$$

The condition for existence and uniqueness of bounded solutions developed in Appendix B is that $\theta_{FW} = \|\bar{\Delta}\|\exp(\|\bar{\mathcal{K}}\|) < 1$.

Given a condition for existence and uniqueness of bounded solutions, we must now compute the values of $\|\bar{\mathcal{K}}\|$ and $\|\bar{\Delta}\|$. First, a bound on the norm of $\bar{\mathcal{K}}$ is computed by

$$\|\bar{\mathcal{K}}\|(\kappa) \leqslant \sup_{\substack{\zeta\in[0,Z/L_H]\\ \tau\in(0,\infty)}} 2\tau\int_{\zeta}^{Z/L_H} \mathrm{d}\zeta'\,\tilde{\alpha}(\zeta') \times\left|\sin\left[\frac{\kappa^2}{2}(\zeta-\zeta')\right]\right| e^{-1/2\kappa^2 D_{\bar{w}}(\zeta,\zeta')\tau^2}$$

$$\leqslant \max_{\tau\in(0,\infty)} 2\tau\int_{0}^{Z/L_H} \mathrm{d}\zeta'\,\tilde{\alpha}(\zeta') \times\left|\sin\left[\frac{\kappa^2}{2}\zeta'\right]\right| e^{-1/2\kappa^2 C_V^2 L_H^{2/3}/v_0^2\zeta'^{2/3}\tau^2}. \quad (105)$$

Similarly compute a bound on the norm of $\bar{\Delta}$ as

$$\|\bar{\Delta}\|(\kappa) \leqslant \sup_{\substack{\zeta\in[0,Z/L_H]\\ \tau\in(0,\infty)}} 4\frac{L_H}{ct_0}\int_0^{\zeta} \mathrm{d}\zeta'\,\zeta'\tilde{\alpha}(\zeta') \times\left|\sin\left[\frac{\kappa^2}{2}(\zeta-\zeta')\right]\right| e^{-1/2\kappa^2 D_{\bar{w}}(\zeta,\zeta')\tau^2} \quad (106)$$

$$\leqslant 4\frac{L_H}{ct_0}\int_0^{Z/L_H} \mathrm{d}\zeta'\,\zeta'\tilde{\alpha}(\zeta')\left|\sin\left[\frac{\kappa^2}{2}(Z/L_H-\zeta')\right]\right|. \quad (107)$$

Our approach for consideration of approximations to $\theta_{FW}(\kappa)$ is quite different from that for $\theta_{PO}(\kappa)$. The Marechal approximation provides a grossly conservative result. The difficulty in use of the Marechal approximation arises from the competing influence of the sine and exponential functions in calculation of the maximum over τ in $\|\bar{\mathcal{K}}\|(\kappa)$. As a result, we adopt an approach of developing a workable approximation that eliminates the need for numerical optimization over τ, given that the optimization over ζ was trivial to evaluate. This will allow the solution, although complex and not obviously intuitive, to be expressed as a function of κ strictly in terms of key scaling constants and moments of the absorption profile.

The approach that follows is to form an approximation for $\|\bar{\mathcal{K}}\|(\kappa)$ based on a third-order expansion of the exponential function in the expression for $\|\bar{\mathcal{K}}\|(\kappa)$. This allows us to then approximately compute the value τ that maximizes $\|\bar{\mathcal{K}}\|(\kappa)$ for each value of κ. This resultant value of τ is then substituted back into the expression for $\|\bar{\mathcal{K}}\|(\kappa)$ to obtain the final result. The expression for $\|\bar{\mathcal{K}}\|(\kappa)$ can be approximately written as

$$\|\bar{\mathcal{K}}\|(\kappa) \leqslant \tau_{\mathcal{K}} 2\frac{Z}{L_H}\mu_{\tilde{\alpha},S}\left(\frac{\kappa^2}{2}\right) - \tau_{\mathcal{K}}^3\kappa^2\frac{C_V^2Z^{2/3}}{v_0^2}\frac{Z}{L_H}\mu_{\tilde{\alpha},S,2/3}\left(\frac{\kappa^2}{2}\right) + \tau_{\mathcal{K}}^5\frac{1}{4}\kappa^4\left(\frac{C_V^2Z^{2/3}}{v_0^2}\right)^2\frac{Z}{L_H}\mu_{\tilde{\alpha},S,4/3}\left(\frac{\kappa^2}{2}\right) - \tau_{\mathcal{K}}^7\frac{1}{24}\kappa^6\left(\frac{C_V^2Z^{2/3}}{v_0^2}\right)^3\frac{Z}{L_H}\mu_{\tilde{\alpha},S,2}\left(\frac{\kappa^2}{2}\right)$$

$$\mu_{\tilde{\alpha},S,\nu}(a) = \int_0^1 \mathrm{d}\zeta'\,\zeta'^{\nu}\tilde{\alpha}\left(\zeta'\frac{Z}{L_H}\right)\sin\left(a\zeta'\frac{Z}{L_H}\right), \quad (108)$$

where $\tau_{\mathcal{K}}$ is the solution to maximization over τ. Optimization over τ is performed by taking the derivative of the above expression with respect to τ and solving the resultant cubic polynomial for the smallest positive real root. This calculation is relatively straightforward given the information provided in this paper. Given the value for $\tau_{\mathcal{K}}$ we can summarize our expression for $\|\bar{\mathcal{K}}\|(\kappa)$ as

$$\|\bar{\mathcal{K}}\|(\kappa) \leqslant 2\tau_{\mathcal{K}}\int_0^{Z/L_H} \mathrm{d}\zeta'\,\tilde{\alpha}(\zeta')\left|\sin\left[\frac{\kappa^2}{2}\zeta'\right]\right| e^{-1/2\kappa^2 D_{\bar{w}}(0,\zeta')\tau_{\mathcal{K}}^2}. \quad (109)$$

The reader will note we have returned to the more general form for the structure function of aberrations, implicitly suggesting that the Kolmogorov approximation be used for calculation of $\tau_{\mathcal{K}}$, but an arbitrary structure function could be used if desired for calculation of $\|\bar{\mathcal{K}}\|(\kappa)$.

In Fig. 2 we provide the resultant exact and approximate values for the maximum value of η_0 that is permissible for phase and full-wave compensation for an example 8 km propagation scenario (this is relevant for determining the time of flight). The exact calculation method and the approximate calculation method for θ_{FW} are used. The reader will observe that the approximate method is accurate up to the minimum value for η_0. This is all that is practically required: if a system is stable at higher spatial frequencies, then it must also be stable at the spatial frequency corresponding to the minimum value of η_0; that is the system must be stable at all spatial frequencies in the range $[\ell_f/D, \ell_f/\ell]$ in order for one to consider the system stable.

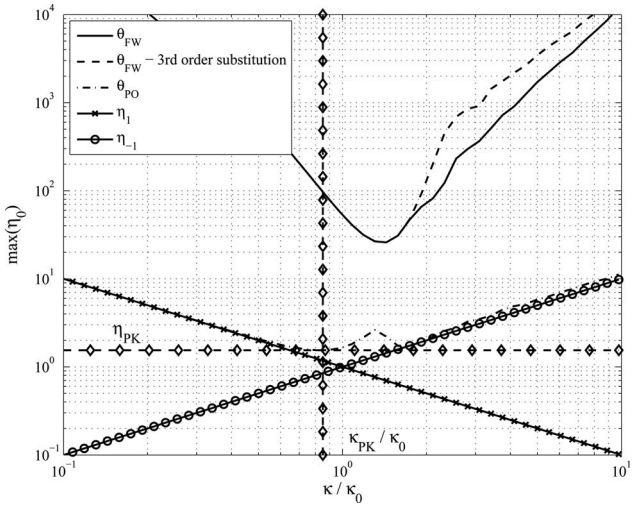

Fig. 2. Calculation of the API parameter η_0 as a function of normalized spatial frequency κ/κ_0 to ensure stability for phase and full-wave compensation. The figure provides asymptotic bounds for the phase compensation case. The figure provides the result based both on exact calculation of θ_{FW} and on approximate calculation of θ_{FW}. The agreement of the two methods is very good up to the minimum value of η_0, which is all that is practically required

Figure 2 illustrates a primary conclusion that can be drawn: full-wave compensation offers at least an order of magnitude improvement in stability margin relative to phase compensation. This translates into an order of magnitude higher power levels that can be tolerated or an order of magnitude higher absorption that can be tolerated, or an appropriate combination of the two. The reader should note that if compensation is required only at spatial scales well below κ_0, then the advantage of full-wave compensation can be two or three orders of magnitude. An important question raised by a reviewer is in regard to the impact of increasing the range. Clearly this increases the impact of time of flight. By the time the range doubles, the impact of time of flight is such that the advantages at the peak frequency have eroded. The advantages can be recovered by a corresponding reduction in the absorption or power level. In addition, advantages of full-wave compensation remain at low spatial frequencies; thus in application of the theory developed in this paper, one must study each problem of interest in detail to understand the trade space.

6. DISCUSSION

This paper provides a theoretical treatment for examination of compensation of thermal blooming and turbulence. The primary results developed are stability boundaries for phase and full-wave conjugation. In the case of full-wave conjugation, the only mechanism to induce instability is laser time of flight. The bounds are conservative, but provide a good understanding of the primary effects involved that induce instability in thermal blooming compensation. The fact that compensation instability can be induced by time of flight even when using full-wave conjugation is an interesting result, indicating a need to accurately model laser time of flight when considering compensation of laser beams for the effects of thermal blooming and turbulence. Example results using the stability bounds developed indicate that full-wave compensation has a greater region of stability than phase compensation.

The reader should note that the results developed herein do not replace wave optical simulation evaluation of the impact of compensation instability on thermal blooming compensation. Instead, they provide motivation for developing a better understanding of the underlying phenomena. Further studies should include detailed numerical evaluation of the accuracy of the theory to determine its direct relevance. In addition, effects such as finite compensation bandwidth affect the onset of PCI. Essentially the use of a finite compensation bandwidth reduces the norms used in computation of the stability boundaries, which corresponds to a reduced probability of the onset of compensation instability.

APPENDIX A

In this appendix, we provide derivation of a fairly standard application of the contraction mapping theorem to prove existence and uniqueness of solutions of an integration equation. Normally we would consider this to be an elementary and ancillary result; however, many in the audience will find this technique unfamiliar, and it is important to provide this background to motivate interest in the innovative and interesting technique derived in Appendix B. Define the integral operator associated with phase-only compensation,

$$T_{PO}[\chi_H(\bar{\kappa},\zeta,\tau)] = \mathcal{M}[\chi_H(\bar{\kappa},\zeta,\tau)] + \tilde{\chi}_{\mathcal{H}}(\bar{\kappa},\zeta,\tau), \tag{A1}$$

and consider solutions to the equation

$$T_{PO}[\chi_H(\bar{\kappa},\zeta,\tau)] = \chi_H(\bar{\kappa},\zeta,\tau), \tag{A2}$$

where $\zeta \in [0, Z/L_H]$ and $\tau \in [0,T]$. Bounded solutions for all $T \in [0,\infty]$ are desired. Define the space of interest X to be the space of continuous functions defined on ζ and τ, $X = \mathcal{C}([0, Z/L_H] \times [0,T])$.

Define M_0 as

$$M_0 = \max_{\zeta\in[0,Z/L_H],\tau\in[0,\infty]} |\tilde{\chi}_{\mathcal{H}}(\bar{\kappa},\zeta,\tau)|. \tag{A3}$$

Using the definition for M_0, one can define a set in X,

$$\Omega = \left\{ (\zeta,\tau,u) | \zeta \in [0,Z/L_H], \tau \in [0,T], |u| \leqslant \frac{M_0}{1-\theta_{PO}} \right\}. \tag{A4}$$

All values of u in Ω correspond to bounded functions in the space X. Consider the closed set $\Omega_0 \subset \Omega$,

$$\Omega_0 = \left\{ (\zeta,\tau,u) | \zeta \in [0,Z/L_H], \tau \in [0,T], |u - \mathcal{L}^{-1}(\mathcal{M}_0\{\mathcal{L}[\tilde{n}_T(\bar{\kappa},\zeta,\tau)]\})| \leqslant \frac{\theta_{PO}}{1-\theta_{PO}} M_0 \right\}. \tag{A5}$$

Examination of Ω_0 motivates the definition of a closed set $Y \subset X$,

$$Y = \left\{ \chi_H(\bar{\kappa},\zeta,\tau) \in X \middle| |\chi_H(\bar{\kappa},\zeta,\tau) - \mathcal{L}^{-1}(\mathcal{M}_0\{\mathcal{L}[\tilde{n}_T(\bar{\kappa},\zeta,\tau)]\})| \leqslant \frac{\theta_{PO}}{1-\theta_{PO}} M_0 \right\}. \tag{A6}$$

It is clear that $T_{PO}: Y \to Y$ for all $\chi_H(\bar{\kappa},\zeta,\tau) \in Y$:

$$\|T_{PO}[\chi_H(\bar{\kappa},\zeta,\tau)] - \mathcal{L}^{-1}(\mathcal{M}_0\{\mathcal{L}[\tilde{n}_T(\bar{\kappa},\zeta,\tau)]\})\| = \|\mathcal{M}[\chi_H(\bar{\kappa},\zeta,\tau)]\| \tag{A7}$$

$$\leqslant \|\mathcal{M}\| \|\chi_H(\bar{\kappa},\zeta,\tau)\| \tag{A8}$$

$$\leqslant \theta_{PO} \frac{M_0}{1-\theta_{PO}}, \tag{A9}$$

and thus $T_{PO}[\chi_H(\bar{\kappa},\zeta,\tau)] \in Y$. Next, it is clear that T_{PO} is a contraction; for all $\chi_{H,1}(\bar{\kappa},\zeta,\tau) \in Y$, $\chi_{H,2}(\bar{\kappa},\zeta,\tau) \in Y$,

$$\|T_{PO}[\chi_{H,1}(\bar{\kappa},\zeta,\tau)] - T_{PO}[\chi_{H,2}(\bar{\kappa},\zeta,\tau)]\| = \|\mathcal{M}[\chi_{H,1}(\bar{\kappa},\zeta,\tau) - \chi_{H,2}(\bar{\kappa},\zeta,\tau)]\| \tag{A10}$$

$$\leqslant \|\mathcal{M}\| \|\chi_{H,1}(\bar{\kappa},\zeta,\tau) - \chi_{H,2}(\bar{\kappa},\zeta,\tau)\| \tag{A11}$$

$$\leqslant \theta_{PO} \|\chi_{H,1}(\bar{\kappa},\zeta,\tau) - \chi_{H,2}(\bar{\kappa},\zeta,\tau)\| \tag{A12}$$

$$< \|\chi_{H,1}(\bar{\kappa},\zeta,\tau) - \chi_{H,2}(\bar{\kappa},\zeta,\tau)\|. \tag{A13}$$

Now, applying the contraction mapping theorem, for $\theta_{PO} < 1$, solutions to the average equation exist that are bounded and unique.

APPENDIX B

In this appendix, we develop a method for application of the contraction mapping theorem to the operator describing full-wave conjugation including time of flight. In general, this appendix provides an interesting method for use of the contraction mapping theorem in consideration of perturbations to Volterra integral operators:

$$T_{FW}[\chi_H(\bar{\kappa},\zeta,\tau)] = \bar{\mathcal{K}}[\chi_H(\bar{\kappa},\zeta,\tau)] + \bar{\Delta}[\chi_H(\bar{\kappa},\zeta,\tau)] + \tilde{\chi}_H(\bar{\kappa},\zeta,\tau). \tag{B1}$$

Assume that $\bar{\mathcal{K}}$ is Volterra. We seek unique, bounded solutions to $T_{FW}[\chi_H(\bar{\kappa},\zeta,\tau)] = \chi_H(\bar{\kappa},\zeta,\tau)$ in a closed set in X. Take the space $X = C([0, Z/L_H] \times [0, T])$ and note that the following property can be shown to be true quite easily using the fact that $\bar{\mathcal{K}}$ is Volterra:

$$\|\bar{\mathcal{K}}^n u\| \leq \frac{\|\bar{\mathcal{K}}\|^n}{n!}\|u\|. \tag{B2}$$

Assume that $\|\bar{\Delta}\|\exp(\|\bar{\mathcal{K}}\|) \leq \theta_{FW} - \varepsilon < 1 - \varepsilon$ and that N is selected such that $\|\bar{\mathcal{K}}\|^N/N! \leq \varepsilon/2$. Then, operating on $T[\chi_H(\bar{\kappa},\zeta,\tau)] = \chi_H(\bar{\kappa},\zeta,\tau)$ with $\Sigma_{k=0}^{N}\bar{\mathcal{K}}^n[\chi_H(\bar{\kappa},\zeta,\tau)]$, obtain

$$\begin{aligned}\sum_{k=0}^{N}\bar{\mathcal{K}}^n[\chi_H(\bar{\kappa},\zeta,\tau)] &= \sum_{k=1}^{N+1}\bar{\mathcal{K}}^n[\chi_H(\bar{\kappa},\zeta,\tau)] + \sum_{k=0}^{N}\bar{\mathcal{K}}^n\bar{\Delta}[\chi_H(\bar{\kappa},\zeta,\tau)] \\ &\quad + \sum_{k=0}^{N}\bar{\mathcal{K}}^n[\mathcal{L}^{-1}(\mathcal{M}_0\{\mathcal{L}[\tilde{n}_T(\bar{\kappa},\zeta,\tau)]\})],\end{aligned}$$

$$\begin{aligned}\chi_H(\bar{\kappa},\zeta,\tau) &= \bar{\mathcal{K}}^{N+1}[\chi_H(\bar{\kappa},\zeta,\tau)] + \sum_{k=0}^{N}\bar{\mathcal{K}}^n\bar{\Delta}[\chi_H(\bar{\kappa},\zeta,\tau)] \\ &\quad + \sum_{k=0}^{N}\bar{\mathcal{K}}^n[\mathcal{L}^{-1}(\mathcal{M}_0\{\mathcal{L}[\tilde{n}_T(\bar{\kappa},\zeta,\tau)]\})] \\ &= S_N[\chi_H(\bar{\kappa},\zeta,\tau)].\end{aligned} \tag{B3}$$

Given the fact that $\Sigma_{k=0}^{N}\bar{\mathcal{K}}^n$ is one to one and onto, solving $S_N[\chi_H(\bar{\kappa},\zeta,\tau)] = \chi_H(\bar{\kappa},\zeta,\tau)$ is equivalent to solving $T_{FW}[\chi_H(\bar{\kappa},\zeta,\tau)] = \chi_H(\bar{\kappa},\zeta,\tau)$.

The procedure for applying the contraction mapping theorem to $S_N[\chi_H(\bar{\kappa},\zeta,\tau)] = \chi_H(\bar{\kappa},\zeta,\tau)$ is very similar to that for the phase conjugation case. The first step is to define M_1:

$$M_1 = \max_{\zeta\in[0,Z/L_H],\tau\in[0,\infty]}\left|\sum_{k=0}^{N}\bar{\mathcal{K}}^n[\mathcal{L}^{-1}(\mathcal{M}_0\{\mathcal{L}[\tilde{n}_T(\bar{\kappa},\zeta,\tau)]\})]\right|. \tag{B4}$$

Using the definition for M_0, one can define a set in X:

$$\Omega = \left\{(\zeta,\tau,u)|\zeta\in[0,Z/L_H],\tau\in[0,T],|u| \leq \frac{M_1}{1-\theta_{FW}}\right\}. \tag{B5}$$

All values of u in Ω correspond to bounded, continuous functions in the space X. Consider the closed set $\Omega_1 \subset \Omega$:

$$\Omega_1 = \left\{(\zeta,\tau,u)|\zeta\in[0,Z/L_H],\tau\in[0,T], \times\left|u - \sum_{k=0}^{N}\bar{\mathcal{K}}^n\mathcal{L}^{-1}(\mathcal{M}_0\{\mathcal{L}[\tilde{n}_T(\bar{\kappa},\zeta,\tau)]\})\right| \leq \frac{\theta_{FW}}{1-\theta_{FW}}M_1\right\}. \tag{B6}$$

Examination of Ω_1 motivates the definition of a closed set $Y \subset X$:

$$Y = \left\{\chi_H(\bar{\kappa},\zeta,\tau)\in X\middle|\ \chi_H(\bar{\kappa},\zeta,\tau) - \sum_{k=0}^{N}\bar{\mathcal{K}}^n\mathcal{L}^{-1}(\mathcal{M}_0\{\mathcal{L}[\tilde{n}_T(\bar{\kappa},\zeta,\tau)]\})\right| \leq \frac{\theta_{FW}}{1-\theta_{FW}}M_1\right\}. \tag{B7}$$

For convenience, denote

$$\chi_0(\bar{\kappa},\zeta,\tau) = \mathcal{L}^{-1}(\mathcal{M}_0\{\mathcal{L}[\tilde{n}_T(\bar{\kappa},\zeta,\tau)]\}).$$

We now show that $S_N: Y \to Y$ for all $\chi_H(\bar{\kappa},\zeta,\tau)\in Y$:

$$\left\|S_N[\chi_H(\bar{\kappa},\zeta,\tau)] - \sum_{k=0}^{N}\bar{\mathcal{K}}^n[\chi_0(\bar{\kappa},\zeta,\tau)]\right\| = \left\|\bar{\mathcal{K}}^{N+1}[\chi_H(\bar{\kappa},\zeta,\tau)] + \sum_{n=0}^{N}\bar{\mathcal{K}}^n\bar{\Delta}[\chi_H(\bar{\kappa},\zeta,\tau)]\right\| \tag{B8}$$

$$\leq \|\bar{\mathcal{K}}^{N+1}[\chi_H(\bar{\kappa},\zeta,\tau)]\| + \|\bar{\Delta}\|\sum_{n=0}^{N}\|\bar{\mathcal{K}}^n[\chi_H(\bar{\kappa},\zeta,\tau)]\| \tag{B9}$$

$$\leq \frac{\|\bar{\mathcal{K}}\|^{N+1}}{(N+1)!}\frac{M_1}{1-\theta_{FW}} + \|\bar{\Delta}\|\sum_{n=0}^{N}\frac{\|\bar{\mathcal{K}}\|^n}{n!}\frac{M_1}{1-\theta_{FW}} \tag{B10}$$

$$\leq [\varepsilon/2 + \|\bar{\Delta}\|\exp(\|\bar{\mathcal{K}}\|)]\frac{M_1}{1-\theta_{FW}} \tag{B11}$$

$$\leq \left(\theta_{FW} - \frac{\varepsilon}{2}\right)\frac{M_1}{1-\theta_{FW}} \tag{B12}$$

$$< \theta_{FW}\frac{M_1}{1-\theta_{FW}}, \tag{B13}$$

and thus $S_N[\chi_H(\bar{\kappa},\zeta,\tau)]\in Y$.

Next, using the same calculation, one can show that S_N is a contraction: for all $\chi_{H,1}(\bar{\kappa},\zeta,\tau)\in Y$, $\chi_{H,2}(\bar{\kappa},\zeta,\tau)\in Y$,

$$\begin{aligned}&\|S_N[\chi_{H,1}(\bar{\kappa},\zeta,\tau)] - S_N[\chi_{H,2}(\bar{\kappa},\zeta,\tau)]\| \\ &\quad = \|S_N[\chi_{H,1}(\bar{\kappa},\zeta,\tau) - \chi_{H,2}(\bar{\kappa},\zeta,\tau)]\|\end{aligned} \tag{B14}$$

$$\times \left\| \bar{\mathcal{K}}^{N+1}[\chi_{H,1}(\bar{\kappa},\zeta,\tau) - \chi_{H,2}(\bar{\kappa},\zeta,\tau)] + \sum_{n=0}^{N} \bar{\mathcal{K}}^{n}\bar{\Delta}[\chi_{H,1}(\bar{\kappa},\zeta,\tau) - \chi_{H,2}(\bar{\kappa},\zeta,\tau)] \right\| \leq \|\bar{\mathcal{K}}^{N+1}[\chi_{H,1}(\bar{\kappa},\zeta,\tau) - \chi_{H,2}(\bar{\kappa},\zeta,\tau)]\| \tag{B15}$$

$$+ \|\bar{\Delta}\| \sum_{n=0}^{N} \|\bar{\mathcal{K}}^{n}[\chi_{H,1}(\bar{\kappa},\zeta,\tau) - \chi_{H,2}(\bar{\kappa},\zeta,\tau)]\| \tag{B16}$$

$$\leq \left(\frac{\|\bar{\mathcal{K}}\|^{N+1}}{(N+1)!} + \|\bar{\Delta}\| \sum_{n=0}^{N} \frac{\|\bar{\mathcal{K}}\|^{n}}{n!} \right) \|\chi_{H,1}(\bar{\kappa},\zeta,\tau) - \chi_{H,2}(\bar{\kappa},\zeta,\tau)\| \tag{B17}$$

$$\leq [\epsilon + \|\bar{\Delta}\| \exp(\|\bar{\mathcal{K}}\|)] \|\chi_{H,1}(\bar{\kappa},\zeta,\tau) - \chi_{H,2}(\bar{\kappa},\zeta,\tau)\| \tag{B18}$$

$$\leq (\epsilon + \theta_{FW}) \|\chi_{H,1}(\bar{\kappa},\zeta,\tau) - \chi_{H,2}(\bar{\kappa},\zeta,\tau)\| \tag{B19}$$

$$< \|\chi_{H,1}(\bar{\kappa},\zeta,\tau) - \chi_{H,2}(\bar{\kappa},\zeta,\tau)\|. \tag{B20}$$

Now, applying the contraction mapping theorem, for $\theta_{FW} < 1-\varepsilon$, solutions to the average equation exist that are bounded and unique.

ACKNOWLEDGMENTS

The work reported in this paper was supported by the High Energy Laser Joint Technology Office (HEL-JTO) under contract FA9451-04-C-0182. The author sincerely appreciates HEL-JTO support in completion of this work. The original version of this work was developed while the author was an employee of Science Applications International Corporation (SAIC). The original manuscript utilized a less rigorous treatment of the effects of microscale random wind shear and was never submitted for publication due to concerns on the part of the author regarding the approach utilized. The author is grateful for feedback from experts such as Fred White, David Lyman, and Russell Vernon, whose historical background in the area of thermal blooming contributed to the author's understanding of the phenomena of the problem of PCI and thermal blooming. Finally, I thank the reviewer of the paper, who made several comments that have improved the quality of the paper.

REFERENCES

1. L. C. Bradley and J. Herrmann, "Phase compensation for thermal blooming," Appl. Opt. **13**, 331–334 (1974).
2. D. G. Fouche, C. Higgs, and C. F. Pearson, "Scaled atmospheric blooming experiments (SABLE)," Lincoln Lab. J. **5**, 273–292 (1992).
3. R. Holmes, R. Myers, and C. Duzy, "A linearized theory of transient laser heating in fluids," Phys. Rev. A **44**, 6862–6876 (1991).
4. C. A. Primmerman, D. V. Murphy, D. A. Page, B. G. Zollars, and H. T. Barclay, "Compensation of atmospheric optical distortion using a synthetic beacon," Nature (London) **353**, 141–143 (1991).
5. R. Q. Fugate, D. L. Fried, G. A. Ameer, B. R. Boeke, S. L. Browne, P. H. Roberts, R. E. Ruane, G. A. Tyler, and L. M. Wopat, "Measurement of atmospheric wavefront distortion using scattered light from a laser guide star," Nature (London) **353**, 144–146 (1991).
6. R. V. Shack and B. C. Platt, "Production and use of a lenticular Hartmann screen," J. Opt. Soc. Am. **61**, 656 (1971). 1971 OSA Spring Meeting Abstract: http://www.opticsinfobase.org/josa/abstract.cfm?uri=josa-61-5-648.
7. D. L. Fried, "Branch cuts in the phase function," Appl. Opt. **31**, 144–146 (1992).
8. D. L. Fried, "Branch point problem in adaptive optics," J. Opt. Soc. Am. A **15**, 2759–2768 (1998).
9. D. L. Fried, "Adaptive optics wave function reconstruction and phase unwrapping when branch points are present," Opt. Commun. **200**, 43–72 (2002).
10. J. D. Barchers, D. L. Fried, and D. J. Link, "Evaluation of the performance of Hartmann sensors in strong scintillation," Appl. Opt. **41**, 1012–1021 (2002).
11. J. D. Barchers, D. L. Fried, and D. J. Link, "Evaluation of the performance of a shearing interferometer in strong scintillation," Appl. Opt. **41**, 3674–3684 (2002).
12. J. D. Barchers and T. A. Rhoadarmer, "Evaluation of phase shifting approaches for a point diffraction interferometer using the mutual coherence function," Appl. Opt. **41**, 7499–7509 (2002).
13. T. J. Karr, "Thermal blooming compensation instabilities," J. Opt. Soc. Am. A **6**, 1038–1048 (1989).
14. D. L. Fried and R. K.-H. Szeto, "Wind-shear induced stabilization of PCI," J. Opt. Soc. Am. A **15**, 1212–1226 (1998).
15. R. A. Gonsalver, "Compensation of scintillation with a phase-only adaptive optic," Opt. Lett. **22**, 588–590 (1997).
16. M. C. Roggemann and D. J. Lee. "A deformable mirror concept for correcting scintillation effects in laser beam projection through the atmosphere," Appl. Opt. **37**, 4577–4485 (1998).
17. J. D. Barchers and B. L. Ellerbroek, "Improved compensation of turbulence induced amplitude and phase distortions by means of multiple near field phase adjustments," J. Opt. Soc. Am. A **18**, 399–411 (2001).
18. J. D. Barchers "Evaluation of the impact of finite resolution effects on scintillation compensation using two deformable mirrors," J. Opt. Soc. Am. A **18**, 3098–3109 (2001).
19. J. D. Barchers "Application of the parallel generalized projection algorithm to the control of two finite resolution deformable mirrors for scintillation compensation," J. Opt. Soc. Am. A **19**, 54–63 (2002).
20. J. D. Barchers, "Closed loop stable control of two deformable mirrors for compensation of amplitude and phase fluctuations," J. Opt. Soc. Am. A **19**, 926–945 (2002).
21. P. Sprangle, J. Penano, and B. Hafizi, "Optimum wavelength and power for efficient laser propagation in various atmospheric environments," J. Directed Energy **2**, 71–95 (2006).
22. R. J. Sasiela, *Electromagnetic Wave Propagation in Turbulence* (Springer-Verlag, 1994).